

A multi-control climate policy process for a trusted decision maker

Henri F. Drake^{a,b}, Ronald L. Rivest^{a,1}, Alan Edelman^a, and John Deutch^a

^aMassachusetts Institute of Technology, 77 Massachusetts Ave, Cambridge, MA 02139, USA; ^bMIT-WHOI Joint Program in Oceanography/Applied Ocean Science & Engineering, Cambridge and Woods Hole, MA, 02139, USA

This manuscript was compiled on May 22, 2020

1 **Persistent greenhouse gas (GHG) emissions threaten global climate**
2 **goals (1) and have prompted consideration of climate controls sup-**
3 **plementary to emissions mitigation (2, 3). We present an idealized**
4 **model of optimally-controlled climate change (based on 4), which is**
5 **complementary to simpler analytical models (5) and more compre-**
6 **hensive Integrated Assessment Models (6). We show that the four**
7 **methods of controlling climate damage– mitigation, carbon dioxide**
8 **removal, adaptation, and solar radiation modification– are not inter-**
9 **changeable, as they enter at different stages of the causal chain that**
10 **connects GHG emissions to climate damages. Early and aggressive**
11 **mitigation is always necessary to stabilize GHG concentrations at**
12 **a tolerable level (7). The most cost-effective way of keeping warm-**
13 **ing below 2°C is a combination of all four controls; omitting so-**
14 **lar radiation modification– a particularly contentious climate control**
15 **(8–10)– increases net control costs by 31%. At low discount rates,**
16 **near-term mitigation and carbon dioxide removal are used to perma-**
17 **rently reduce the warming effect of GHGs. At high discount rates,**
18 **however, GHGs concentrations increase rapidly and future genera-**
19 **tions are required to use solar radiation modification to offset a large**
20 **greenhouse effect. We propose a policy response process wherein**
21 **climate policy decision-makers re-adjust their policy prescriptions**
22 **over time based on evolving climate outcomes and revised model as-**
23 **sumptions. We demonstrate the utility of the process by applying it**
24 **to three hypothetical scenarios in which model biases in 1) baseline**
25 **emissions, 2) geoengineering (CDR and SRM) costs, and 3) climate**
26 **feedbacks are revealed over time and control policies are re-adjusted**
27 **accordingly.**

Climate policy | Mitigation | Adaptation | Geoengineering | Integrated Assessment Model

1 **C**limate change due to anthropogenic greenhouse gas
2 (GHG) emissions poses an existential threat to society
3 (11). Ever since the direct link between GHGs and global
4 warming was established in climate models over fifty years
5 ago (12), scientists have advocated for substantial emissions
6 mitigation to stabilize global GHG concentrations and temper-
7 atures (13). The discovery that humans were unintentionally
8 modifying the climate was unsurprisingly followed by specula-
9 tion about intentional climate control (14). With every year
10 of increasing GHG emissions and climate goals slipping out
11 of reach (1), calls for serious consideration of climate controls
12 beyond just mitigation—and their implications—grow louder
13 (3, 15–18).

14 Four climate controls have emerged as plausible candidates
15 for use in the near future: emissions Mitigation, carbon dioxide
16 Removal (CDR), Geo-engineering by Solar Radiation Modi-
17 fication (SRM), and Adaptation. The four controls are not
18 directly interchangeable as they enter at different stages of the

causal chain of climate damages (Figure 1; 4, 5):

$$\text{Emissions} \xrightarrow{M} \text{GHGs} \xrightarrow{R} \text{Forcing} \xrightarrow{G} \text{Warming} \xrightarrow{A} \text{Damages.} \quad [1]$$

20 Controls further down the chain generally carry greater risks,
21 since they require carefully off-setting the various downstream
22 effects of GHG emissions, but also have advantages: CDR is
23 the only control that decreases GHG concentrations; SRM is
24 quick to deploy and has low direct costs (19); and adaptation
25 allows for flexibility in the other controls as any residual climate
26 damages can be reduced by adapting to the new climate, to
27 some extent (20).
28

29 Numerous social or geopolitical factors may substantially
30 limit or block deployments of certain controls: problems related
31 to inequity (21), distrust (22, 23), or lack of governance (24, 25)
32 are just a handful of examples. Here, we ignore many of these
33 complexities—except in as much they are implicitly included
34 in costs and socio-technological constraints—and focus on the
35 "best-case" scenario where a globally-trusted decision-maker
36 prescribes global control policies and their policy prescriptions
37 are exactly realized.

38 Our hypothetical trusted decision-maker must follow some
39 set of principles on which to base their control policies. Two
40 commonly-studied approaches are 1) the cost-benefit approach
41 (e.g. 26), in which control costs are balanced against the bene-
42 fits of avoided damages, and 2) the cost-effectiveness approach
43 (e.g. 27), in which control costs are minimized subject to a
44 prescribed climate constraint. The cost-effectiveness approach
45 underlies the Paris Climate Agreement (28), which aims to
46 keep global warming well below 2°C above pre-industrial levels
47 and currently organizes global climate policy*.

*Intended nationally determined contributions to this effort imply 2.6–3.1°C of warming and will need to be strengthened at upcoming re-negotiations (and realized) to have a reasonable chance

Significance Statement

We present a simple framework and readily available open source software for optimizing trade-offs between the four primary methods that control human-caused climate damages: 1) reducing anthropogenic greenhouse-gas emissions, 2) removing carbon dioxide from the atmosphere, 3) reducing incoming sunlight through solar radiation modification, and 4) adapting to a changed climate. We describe a policy response process that permits a decision maker to adjust policies and improve model parameters over time based on climate outcomes and research results.

HFD wrote the paper, ran the simulations, and performed the analysis. All authors contributed to the conception of the project, interpretation of the results, and editing of the paper.

¹To whom correspondence should be addressed. E-mail: rivest@mit.edu

48 The conventional tool for optimizing global climate control
 49 are Integrated Assessment Models (IAMs), which are the
 50 result of coupling simple climate system models to simple
 51 energy-economy models (see 30, for a general overview of IAMs
 52 and their utility to date). In this paper, we 1) present an
 53 idealized model of optimally-controlled climate change which
 54 is complementary to both simpler analytical models and more
 55 comprehensive IAMs and 2) we propose a sequential policy
 56 process for periodic and critical re-evaluation of inevitably
 57 biased forecasts, which we illustrate with three hypothetical
 58 examples.

59 MARGO: An idealized model of optimally-controlled cli- 60 mate change

61 The MARGO model consists of a physical energy bal-
 62 ance model of Earth’s climate coupled to an idealized socio-
 63 economic model of climate damages and controls (Figure 1):

- Mitigation of greenhouse gas emissions,
- Adaptation to climate impacts,
- Removal of carbon dioxide (CDR),
- Geoengineering by solar radiation modification (SRM), and
- Optimal deployment of available controls.

65 The model is modular, fast, and customizable and can be run
 66 with several options of objective functions and constraints.

67 Each of the climate controls acts, in its own distinct way,
 68 to reduce the damages caused by a changing climate but carry
 69 their own deployment costs (including direct costs, research
 70 and development costs, infrastructure costs, regulatory costs).
 71 The model is designed to include key features of climate physics,
 72 economics, and policy as concisely as possible and in ways
 73 consistent with both theory and more comprehensive General
 74 Circulation Models and IAMs. The shortcoming of the model’s
 75 simplicity is that while its results provide qualitative insights,
 76 the quantitative results are unreliable.

77 The model is developed in open source using the Julia pro-
 78 gramming language (31) at github.com/hdrake/OptimizeClimate
 79 (Drake et al., 2020). The model originated as an extension of
 80 a previous model (4) to time-dependent control variables, al-
 81 though many improvements have been made since then. Each
 82 model component is expressed in closed form to facilitate
 83 analytical analysis and computation. Unlike most idealized
 84 climate-economic models, the entire MARGO framework can
 85 be explicitly written down in one or two expressions (SI Text
 86 2). A derivation and interpretation of the two-box energy
 87 balance model– which has the same form as that of DICE
 88 (32)– is included in the Methods. The parameter values used
 89 throughout the paper are set to the defaults mentioned in
 90 this section (and comprehensively listed in SI Text 2), except
 91 where explicitly stated otherwise. Validation experiments are
 92 summarized in the Methods and described in detail in the
 93 Supplemental Information.

94 **No-policy baseline scenario.** Climate-controlled scenarios are
 95 considered relative to an exogenous no-policy baseline where
 96 carbon-dioxide equivalent (CO_{2e}) emissions $q(t)$ increase lin-
 97 early four-fold by 2100 relative to 2020 and decrease linearly
 98 to zero by 2150, resulting in 7.3 W/m^2 of radiative forcing
 99 by 2100 and 8.5 W/m^2 by 2150, relative to preindustrial lev-
 100 els. As a result of this forcing, the global-mean temperature

of keeping warming below 2°C (29).

reaches 2°C by 2050 and soars to $T \approx 4.75^\circ \text{C}$ by 2100, relative
 to preindustrial. We interpret this emission scenario as an
 idealized extension of the SSP3 baseline scenario, which is
 characterized by fossil-fueled growth (33).

There are five steps in the causal chain (eq. 1) between
 CO_{2e} emissions and climate damages.

1. CO_{2e} is emitted at a rate $q(t)$, with only a fraction
 $r = 50\%$ (34) remaining in the atmosphere after a few
 years, net of uptake by the ocean and terrestrial biosphere
 (Figure 2a).
2. CO_{2e} concentrations increase as long as the emissions $q(t)$
 are non-zero, and are given by $c(t) = c_0 + \int_{t_0}^t r q(t') dt'$
 (Figure 2b).
3. Increasing CO_{2e} concentrations strengthen the greenhouse
 effect, reducing outgoing longwave radiation and causing
 an increased radiative forcing of $F(t) = a \ln(c(t)/c_0)$,
 which exerts a warming effect on the surface.
4. Near-surface air temperatures eventually increase by
 $T(t) = F(t)/B$ to balance the reduced cooling to space,
 where $B/(\kappa + B) = 60\%$ of the warming occurs within a
 few years and the remaining $\kappa/(\kappa + B) = 40\%$ occurs over
 the course of several centuries due to ocean heat uptake
 (35). The feedback parameter B includes the effects of all
 climate feedbacks, except those involving the carbon cycle
 and the long-term ice sheet response (Figure 2c), and the
 ocean heat uptake rate κ parameterizes the combined
 effects of advection and diffusion of heat into the deep
 ocean.
5. Anthropogenic warming causes a myriad of climate im-
 pacts, which result in damages that increase non-linearly
 with temperature, $D = \beta T^2$.

Effects of climate controls. The four available climate controls
 enter as fractional controls at each link of the climate change
 causal chain (eq. 1).

Mitigation reduces emissions by a factor $M(t) \in [0, 1]$ such
 that the controlled emissions that remain in the atmosphere
 are $r q(t)(1 - M(t))$, where $M = 1$ corresponds to complete
 decarbonization of the economy.

Removal of CO_{2e} , $R(t) \in [0, 1]$, in contrast to mitigation,
 is de-coupled from instantaneous emissions and is expressed
 as the fraction of 2020 baseline emissions that are removed
 from the atmosphere in a given year, $q_0 R(t)$. A maximal value
 of $R = 1$ corresponds to removing $60 \text{ GtCO}_{2e}/\text{year}$, which is
 more than twice a recent upper-bound estimate of the global
 potential for negative emission technologies (36).

A useful diagnostic quantity is the effective emissions

$$r q(t)(1 - M(t)) - q_0 R(t), \quad [2]$$

which is the annual rate of CO_{2e} accumulation in the atmo-
 sphere (Figure 2a), with contributions from both emissions
 mitigation and CDR. The change in CO_{2e} concentrations is
 simply the integral of the effective emissions over time (Figure
 2b),

$$c_{M,R}(t) = c_0 + \int_{t_0}^t r q(t')(1 - M(t')) dt' - q_0 \int_{t_0}^t R(t') dt'. \quad [3]$$

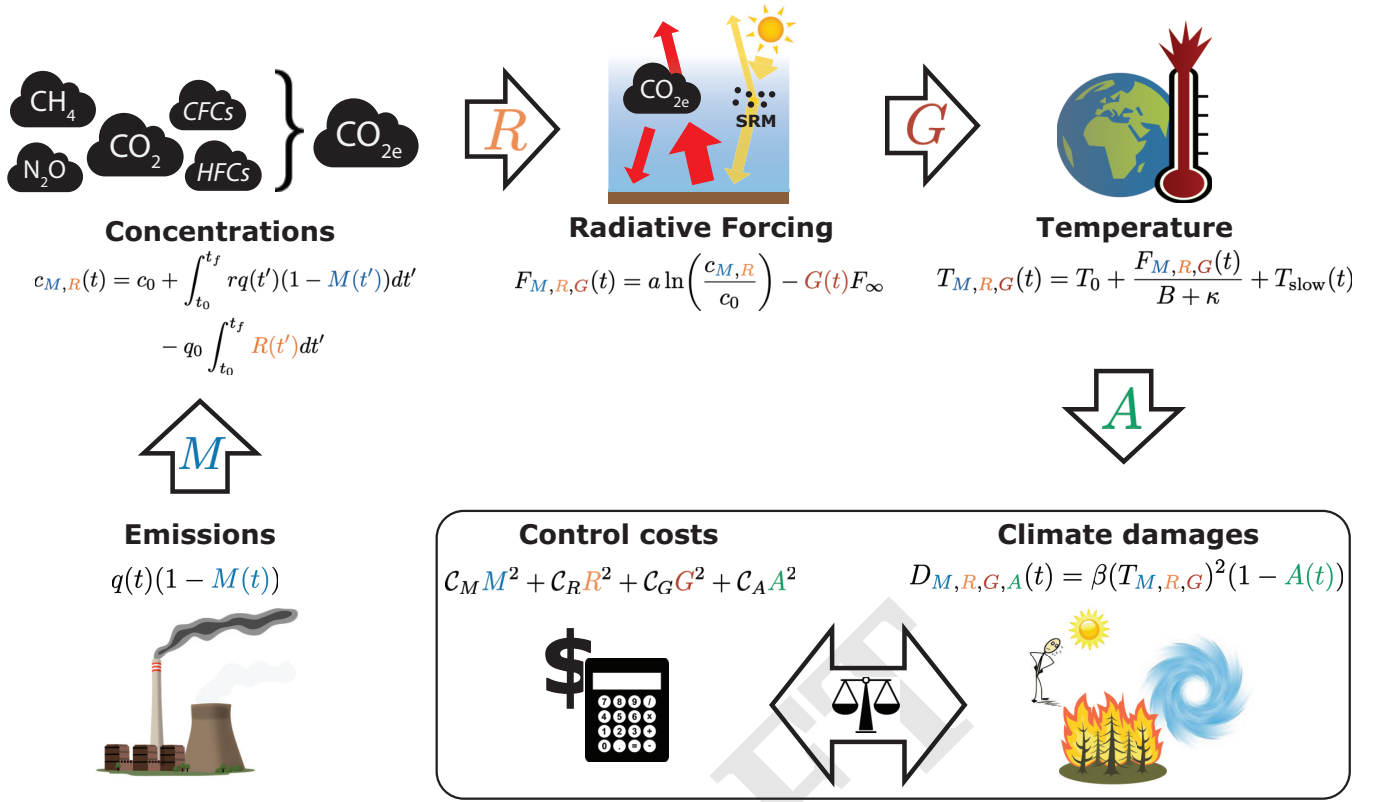


Fig. 1. Schematic of the causal chain from greenhouse gas emissions to climate damages, including the unique effects of four climate controls: emissions Mitigation, carbon dioxide Removal, Geoengineering by Solar Radiation Management (SRM), and Adaptation. Climate controls yield benefits in terms of avoided climate damages, which are balanced against control deployment costs.

154 Geoengineering by SRM, $G(t) \in [0, 1]$, acts to offset a
 155 fraction of the CO_{2e} forcing,

$$156 F_{M,R,G}(t) = F_{M,R}(t) - G(t)F_\infty, \quad [4]$$

157 where $F_{M,R} = a \ln(c_{M,R}(t)/c_0)$ is the controlled CO_{2e} forcing
 158 and $F_\infty = 8.5 \text{ W/m}^2$ is the maximum baseline CO_{2e} forcing,
 159 which is attained starting in 2150, when baseline emissions are
 160 assumed to reach zero. A value of $G = 1$ thus corresponds to a
 161 complete cancellation between the equilibrium warming from
 162 baseline CO_{2e} increases and the cooling from a full deployment
 163 of SRM.

164 The controlled near-surface air temperature (Figure 2c)
 165 evolves according to the total controlled forcing,

$$T_{M,R,G}(t) - T_0 = \frac{F_{M,R,G}(t)}{B + \kappa} + \frac{\kappa}{B} \int_{t_0}^t \frac{e^{-\frac{t-t'}{\tau_D}}}{\tau_D} \frac{F_{M,R,G}(t')}{B + \kappa} dt', \quad [5]$$

166 where $T_0 = 1.1^\circ\text{C}$ is the present warming relative to preindustrial
 167 and $\tau_D = 240$ years is the slow timescale of ocean heat
 168 uptake. The first term on the right-hand side of [5] represents a
 169 fast transient response while the second term represents a
 170 slow recalcitrant response due to the thermal inertia of the
 171 deep ocean (see Methods). Climate inertia decouples the tem-
 172 perature response from instantaneous forcing and implies that
 173 an additional fraction of short-term warming (or cooling) is
 174 locked in for the future, even if radiative forcing is stabilized
 175 (37), as in the case of bringing emissions to zero in our model[†].

[†]In earth system models with a dynamic carbon cycle, the slow recalcitrant warming due to a re-

177 Adaptation to climate impacts acts to reduce damages by a
 178 fraction $A(t) \in [0, 40\%]$. Since some climate impacts are likely
 179 impossible to adapt to (20), we assume that adaptation can
 180 at most reduce climate damages by one-third. The controlled
 181 damages are thus given by

$$182 D_{M,R,G,A} = \beta(T_{M,R,G})^2(1 - A(t)), \quad [6]$$

183 where the damage parameter β is tuned such that a warm-
 184 ing of 3°C results in damages of the 2% of Gross World
 185 Product (GWP), consistent with DICE in the limit of non-
 186 catastrophic warming (32). Although adaptation does not
 187 affect the planetary temperature directly, it is useful to con-
 188 sider an "adapted temperature" $T_{M,R,G,A}$ which yields con-
 189 trolled damages equivalent to the fully-controlled damages
 190 $\beta(T_{M,R,G,A})^2 = \beta(T_{M,R,G})^2(1 - A)$ and is defined

$$191 T_{M,R,G,A} \equiv T_{M,R,G} \sqrt{1 - A}. \quad [7]$$

192 **Costs and benefits of controlling the climate.** The costs of
 193 deploying climate controls are non-negligible and must be
 194 balanced with the benefits of controlling the climate to avoid
 195 climate impact damages. The costs of climate controls are
 196 parameterized as:

$$197 C = C_M M^2 + C_R R^2 + C_G G^2 + C_A A^2, \quad [8]$$

198 where the C_* are the hypothetical annual costs of fully deploy-
 199 ing that control (see Methods) and the cost functions

duction in ocean heat uptake happens to be roughly offset by the ocean carbon sink (34), such that bringing emissions to zero roughly stabilizes temperatures (38). The model's realism would be improved by implementing a simple non-linear model of the ocean carbon cycle (39)

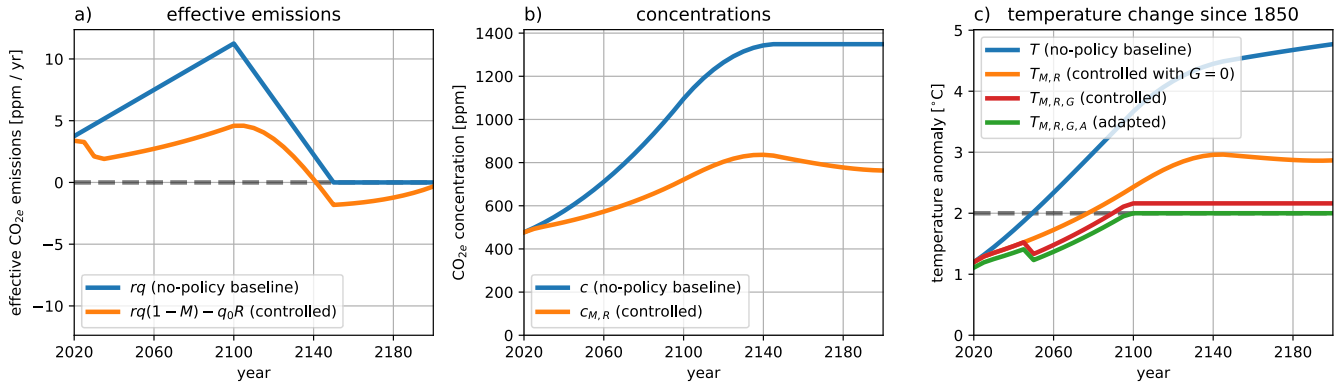


Fig. 2. Baseline (blue) and optimally-controlled (orange) a) effective CO_{2e} emissions, b) CO_{2e} concentrations, and c) temperature anomaly relative to preindustrial from cost-effectiveness analysis. Panel c) shows the optimal temperature change that would occur: in a baseline scenario (blue); with just emissions Mitigation and carbon dioxide Removal (orange); with Mitigation, Removal, and solar-Geoengineering (red); and as an “adapted temperature” (eq. 7) with Adaptation measures also taken into account. The dashed grey line marks the threshold adapted temperature of $T^* = 2^\circ\text{C}$ to be avoided. In (c), $T_{M,R,G}$ and $T_{M,R,G,A}$ decrease slightly in 2050 relative to $T_{M,R}$ as small but non-zero SRM deployment becomes permissible. Equivalent curves for cost-benefit analysis are shown in Figure S1.

200 are assumed to be convex functions of fractional deployment
 201 with zero initial marginal cost, as is customary (5, 6, 26), and
 202 are here all taken to be quadratic for simplicity (4, 5). The
 203 benefits of deploying climate controls are the avoided climate
 204 damages relative to the no-policy baseline scenario,

$$205 \quad \mathcal{B} = D - D_{M,R,G,A} = \beta(T^2 - (T_{M,R,G,A})^2). \quad [9]$$

206 **Exogenous economic growth.** In contrast to conventional
 207 IAMs, which follow classic economic theories of optimal eco-
 208 nomic growth and solve for the maximal welfare based on
 209 the discounted utility of consumption, we here treat economic
 210 growth as exogenous (as in 5). The economy, represented by
 211 the GWP $E(t) = E_0(1 + \gamma)^{(t-t_0)}$, grows from its present value
 212 of $E_0 = 100$ trillion USD with a fixed growth rate $\gamma = 2\%$,
 213 consistent with DICE, expert opinion, and an econometric
 214 forecast model (32, 40). We ignore feedbacks of climate abate-
 215 ment costs and climate damages on economic growth, since
 216 they are small variations relative to the exponential rate of
 217 economic growth in many IAM implementations (32, 41), but
 218 not all (42).

219 Optimal deployments of climate controls

220 A trusted climate policy decision-maker specifies the objective
 221 function to maximize subject to additional policy constraints.
 222 The MARGO model is readily optimized in terms of the time-
 223 dependent climate control variables $M(t), R(t), G(t), A(t)$.
 224 The numerical implementation of the optimization, as well as
 225 additional socio-technological constraints on the permitted
 226 timing and rates of deployments, are described in the Meth-
 227 ods. Here, we describe the optimally-controlled results of two
 228 policy approaches, cost-benefit analysis and cost-effectiveness
 229 analysis, and explore their sensitivity to the discount rate ρ
 230 and possible limits to the fractional penetration of mitigation
 231 μ , respectively.

Cost-benefit analysis. A natural and widely-used approach is
 cost-benefit analysis, in which the cost $\mathcal{C}_{M,R,G,A}$ of deploying
 climate controls is balanced against the benefits $\mathcal{B}_{M,R,G,A}$ of
 the avoided climate damages. Formally, we aim to maximize

the net present benefits:

$$\max \left\{ \int_{t_0}^{t_f} (\mathcal{B}_{M,R,G,A} - \mathcal{C}_{M,R,G,A}) (1 + \rho)^{-(t-t_0)} dt \right\}, \quad [10]$$

where ρ is a social discount rate that determines the annual
 depreciation of future costs and benefits of climate control
 to society. There are different views about the appropriate
 non-zero discount rate to apply to multi-generational social
 utility (43–46). Here, we choose a discount rate of $\rho = 1\%$, on
 the low end of values used in the literature, motivated by our
 preference towards inter-generational equity (47).

The results of maximizing net present benefits are shown in
 Figure 3. Early and aggressive emissions mitigation– and to a
 lesser extent CDR (Fig 3a)– drive net discounted costs of up
 to 1.5 trillion USD/year before 2075 relative to the no-policy
 baseline but deliver orders of magnitude more in net discounted
 benefits from 2075 to 2200 (Fig 3b). Effective CO_{2e} emissions
 reach net-zero by 2040 and concentrations stabilize at $c_{M,R} =$
 500 ppm, slightly above present day $c_0 = 460$ ppm (Figure
 S1a,b). In 2050, deployments of SRM become permissible and
 quickly scale up to a moderate level of $G = 15\%$, permanently
 bringing carbon-controlled temperatures from about $T_{M,R} \approx$
 1.5 °C to $T_{M,R,G} \approx 0.75$ °C above preindustrial (Figure S1c).
 Deployments of adaptation are modest, reflecting its relatively
 high costs and its position at the end of the the causal chain
 of climate damage (eq. 1)

The preference for controls earlier in the causal chain, not-
 ably mitigation, is largely a result of the choice $\rho = 1\%$ for the
 discount rate (Figure 3c). In particular, if the discount rate in-
 creases above the economic growth rate (48), $\rho > \gamma = 2\%$, the
 time decay leads to a different regime of control preferences:
 the short-term fix offered by SRM overwhelmingly becomes the
 preferred control since the high future costs of its unintended
 climate damages are damped by the aggressive discounting of
 future costs. Adaptation emerges as the only control that
 peaks for intermediate values of the discount rate, since its
 benefits are experienced both in the short-term and long-term.

Cost-effectiveness of avoiding damage thresholds. The con-
 ventional cost-benefit approach to understanding climate

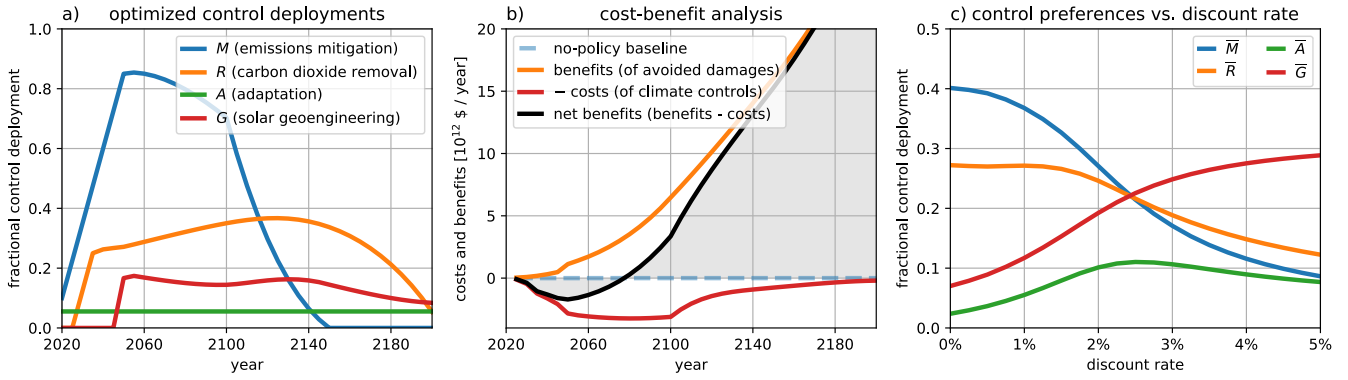


Fig. 3. Results of cost-benefit analysis and sensitivity to the discount rate ρ . (a) Optimal control deployments and (b) corresponding discounted costs and benefits relative to the no climate-policy baseline scenario. The total positive area shaded in grey in (b) is the maximal net present benefits (eq. 10). (c) Time-mean control deployments as a function of the discount rate.

change is limited by the poorly understood damage function (49), which is likely to continue being revised as more is learned about its behavior at high levels of forcing (50, 51). An alternative approach, which presently guides global climate policy negotiations, is to prescribe a threshold of climate damages— or temperatures, as in the Paris Climate Agreement (28)— which is not to be surpassed.

In this implementation, we aim to find the lowest net present costs of control deployments

$$\min \left\{ \int_{t_0}^{t_f} C_{M,R,G,A} (1 + \rho)^{-(t-t_0)} dt \right\} \quad [11]$$

which keep controlled damages below the level corresponding to a chosen temperature threshold, $\beta(T_{M,R,G})^2(1 - A(t)) < \beta(T^*)^2$, which we rewrite

$$T_{M,R,G,A} < T^*, \quad [12]$$

where $T_{M,R,G,A}$ is the "adapted temperature" (eq. 7).

The results of optimizing the cost-effectiveness of controls that keep adapted temperatures below $T^* = 2^\circ\text{C}$ are shown in Figures 2 and 4. Fractional emissions mitigation increases to a maximum of $M = 50\%$ decarbonization by 2035 and is maintained until emissions peak in 2100 (Figures 2a and 4a). Carbon dioxide is initially removed at rate of $Rq_0 \approx 15\% q_0 = 1.1$ ppm/year starting in 2030, which ramps up to $Rq_0 \approx 30\% q_0 = 2.2$ ppm/year by 2140. Since the optimally-controlled temperatures that result from the above cost-benefit analysis are already lower than $T^* = 2^\circ\text{C}$, the optimal controls from cost-effectiveness are less ambitious than for the cost-benefit analysis (Figures 3a, 4a), in contrast to some previous mitigation-only studies (26, 52) but inline with recent analysis (42) that uses an updated climate damage function (51). As a consequence of relatively relaxed mitigation and CDR early on, a sizable deployment of SRM is used to shave off 1°C degree of warming at its peak in the mid-22nd Century in order to meet the temperature goal (Figure 4a and Figure 2c). Adaptation offsets $A = 15\%$ of damages and plays a moderate role in reducing damages to below the threshold. Even with discounting, annual costs of control deployments increase until 2100 and remain roughly constant in the 22nd Century (Figure 4b).

To explore the sensitivity of these results to our assumed mitigation costs $C_M M^2$, which allow for up to 50% mitigation

by 2035 at the relatively low cost of 700 billion USD/year, we compare the results against a re-optimization with steeper costs at high levels of mitigation. The mitigation cost function is modified to

$$C_M M^2 \left(1 - e^{-\left(\frac{1-M}{1-\mu}\right)} \right)^{-1}, \quad [13]$$

where we set the penetration limit of cheap mitigation to $\mu = 40\%$ and the function's structure is shown in Figure 4d. Mitigation costs are unchanged for $M \ll \mu$. Around $M \approx \mu$, low-hanging mitigation options are increasingly exhausted and costs begin to increase much more rapidly than the default assumption M^2 . The high costs of deep decarbonization drive a reduction in the peak mitigation from $M = 50\%$ to nearly $M = 30\%$ in 2060, with the decreased mitigation being compensated by increases in the other three controls (Figure 4c).

Benefits of a complete portfolio of climate controls

To quantify the benefits of considering a complete portfolio of climate controls, as opposed to considering control technologies in isolation, we compute optimal control trajectories with all 15 combinations of the controls $\alpha \in \{M, A, R, G\}$, setting $\alpha \equiv 0$ for omitted technologies. The most cost-effective strategy includes all four controls and has a net present cost of 136 trillion USD (discount rate of $\rho = 1\%$). Since mitigation is the dominant control in the $\{MARG\}$ scenario (Figure 4a), the six most cost-effective portfolios include mitigation, with the no-SRM $\{MAR\}$ and mitigation-plus-CDR $\{MR\}$ scenarios costing only 31% and 38% more than the $\{MARG\}$ scenario, respectively (Table 1). The costs in single-control scenarios are much larger, with additional costs of 136% for the mitigation-only scenario $\{M\}$ to 201% for the SRM-only scenario $\{G\}$. In the adaptation-only $\{A\}$ and CDR-only $\{R\}$ scenarios, there is no solution that avoids an adapted temperature of $T^* = 2^\circ\text{C}$, because we have imposed an adaptability limit $A < 40\%$ (20) and limits to plausible levels of CDR $q_0 R < q_0 = 60$ GtCO_{2e}/year (see Methods).

A policy process for responding to uncertain future outcomes

Integrated Assessment Modelling (IAM) approaches assume perfect foreknowledge of model dynamics, parameters (or pa-

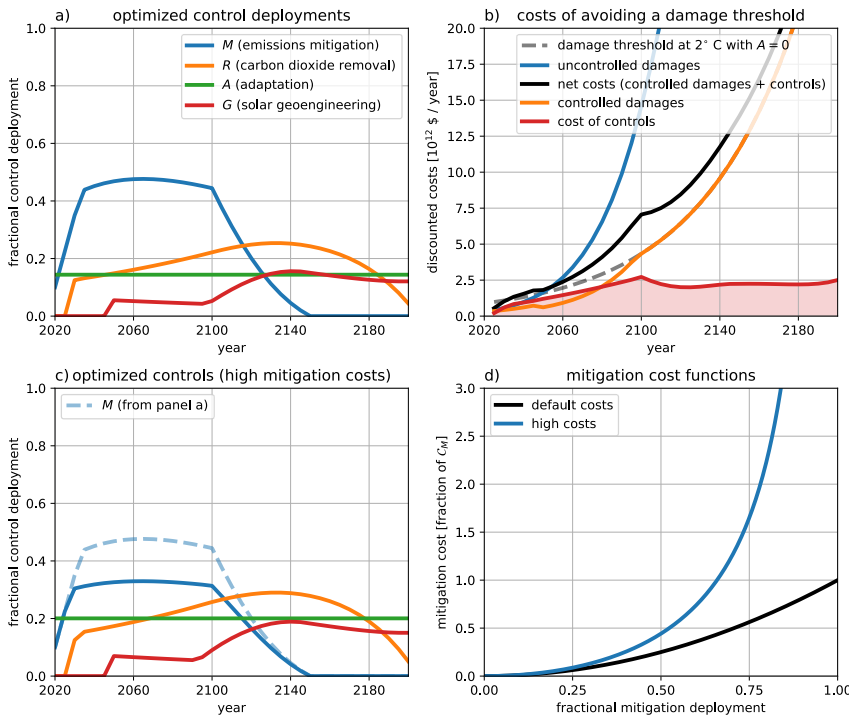


Fig. 4. Results of cost-effectiveness analysis and sensitivity to potential limits μ to mitigation. (a) Optimal control deployments and (b) corresponding costs and damages. In panel (b), the blue line shows the discounted baseline uncontrolled damages; the dashed grey line shows the discounted damages associated with 2° of warming, which are to be avoided at all costs; the orange line shows the discounted damages in the optimally-controlled solution; and the red line shows the optimal discounted costs of controls such that the shaded area below is the minimal net present costs of controls (eq. 11). (c) Control deployments, as in (a), but re-optimized with high costs of deep decarbonization (blue line in d, eq. 13) relative to the default mitigation costs (black line in d). Mitigation in the default scenario (a) is reproduced as a dashed line in (c) for ease of comparison.

Table 1. Additional net present cost of avoiding an adapted temperature of $T^* = 2^\circ\text{C}$, relative to the 136 trillion USD net present cost of controls in the $\{MARG\}$ reference scenario with all four controls available: mitigation (M), adaptation (A), CDR (R) and SRM (G).

MARG	MRG	MAR	MAG	MR	MG	ARG	RG
0%	5%	31%	34%	38%	46%	63%	96%

MA	AG	M	G	AR	R	A	
105%	109%	136%	201%	216%	N/A	N/A	

Since we have imposed upper bounds $A < 40\%$ and $q_0 R < q_0 = 60 \text{ GtCO}_{2e}/\text{year}$ on adaptation and CDR, there is no scenario in which they can, in isolation, keep damages below those associated with $T^* = 2^\circ\text{C}$ of warming.

parameter distributions), and inputs. Future outcomes will differ from projections because the models are imperfect approximations of the socio-economic and physical climate systems they represent. For example, socio-economic models may assume erroneous future costs of climate controls (53) and physical climate models may omit tipping elements (11), both of which would lead to biases in model projections with respect to actual outcomes. Furthermore, the assumption of perfect foreknowledge degrades the active roles of policy decision-makers in determining baselines and control cost functions, and of climate researchers in refining estimates of physical model parameters.

A hypothetical trusted climate policy decision-maker must be in a position to respond to the inevitable differences that arise between model projections and actual outcomes and to revise their system understanding based on the newest developments in research. We show how our model equips climate policy decision-makers with the ability to periodically re-evaluate policy prescriptions by revising the underlying

model structure and parameter values to correct for revealed biases.

The responsive control strategy process we propose is as follows:

1. Initial future trajectories of optimal control deployments are computed from the vantage point of $t = t_0$;
2. Model projections and control deployments are integrated forward one policy-making period to $t_1 = t_0 + \Delta t$;
3. Model structure and parameter values are revised, owing to new information obtained from observed outcomes and research developments;
4. Future trajectories of control deployments are re-optimized, now from the vantage point of $t_1 = t_0 + \Delta t$ and with revised model parameters;
5. Return to step 2, replacing $t_1 = t_0 + \Delta t$ with $t_n = t_{n-1} + \Delta t$ for period n , and repeat the process for the desired number of periods.

To illustrate the utility of the policy response process, we apply it to three hypothetical future scenarios, in which the most cost-effective controls for keeping adapted temperatures below $T^* = 2^\circ\text{C}$ are sequentially re-optimized in response to changes in model inputs and parameters. As a point of reference, we note that the passage of time itself leads to minor adjustments in the optimal combination of control deployments. As each successive generation is exposed to increasingly damaging temperatures, their most cost-effective solution is to increase adaptation measures, which past generations did not yet need, and save costs by slightly decreasing all other controls in the near future (Figure 5a,b). The control adjustments in the three scenarios below (Figure 5c-h) are shown relative to those in the reference case (Figure 5a,b).

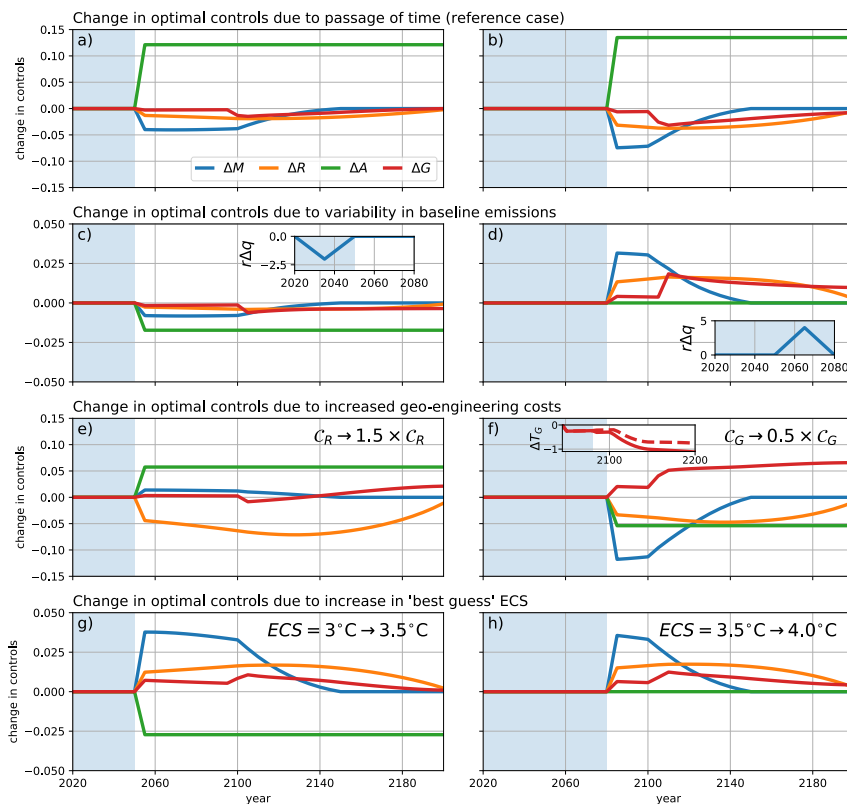


Fig. 5. Illustration of the proposed policy process in which the optimally cost-effective control policies are periodically re-adjusted, relative to the original policies prescribed in 2020 (Figure 4a). In a reference case (a,b), time advances sequentially to 2050 (a) and 2080 (b) and policies are re-adjusted to reflect the new timelines. The blue shading shows the passage of time. The changes in control deployments shown in (c-h) are due to sequential re-optimization at 2050 (left) and 2080 (right), relative to the reference case (a,b), but now with revised model parameters: (c,d) where historical effective emissions $r\Delta q(t)$ are sequentially decreased and then increased (see insets); (e,f) where the costs of CDR and SRM are sequentially increased and decreased, respectively; and (g,h) where the best guess of the Equilibrium Climate Sensitivity (ECS) is revised upwards in 2050 and again in 2080. The inset in (d) shows the cooling due to SRM $\Delta T_G = T_{M,R,G} - T_{M,R}$ in the default scenario (dashed) and after the re-evaluation in 2080 shown in panel (d) (solid).

Scenario 1: revealed bias in projected near-term baseline emissions. Suppose in $t_0 = 2020$ that the policy decision-maker prescribes aggressive climate control policies based on their cost-effectiveness at keeping warming below $T^* = 2^\circ\text{C}$ (step 1; Figure 4a) and that these optimal climate controls are perfectly implemented over the following $\Delta t = 30$ years (step 2).

The policy decision-maker directs a re-evaluation of the optimal control strategy at $t_1 = 2050$. The actual baseline emission trajectory between $t_0 = 2020$ and $t_1 = 2050$ is found to be $r\Delta q = 1$ ppm/year lower than projected on average (Figure 5c, inset), resulting in lower CO_{2e} concentrations than anticipated and a projected maximum warming of $\max(T_{M,R,G,A}) = 1.9^\circ\text{C}$, well below the $T^* = 2^\circ\text{C}$ goal. The model inputs are thus revised to account for these lower-than-expected historical baseline emissions (step 3) and the optimal future control trajectories are re-computed (step 4). Reduced historical emissions imply a larger remaining carbon budget (54) and allow the policy decision-maker to slightly relax control deployments while still remaining below $T^* = 2^\circ\text{C}$ of warming (Figure 5c), resulting in 12 trillion USD of avoided net present control costs. At this point, the policy decision maker must decide whether to continue existing policies that lead to 1.9°C of warming or to reduce future controls deployments (and costs) at the risk of increased climate impacts due to an additional 0.1°C of warming.

Suppose that, after following the re-optimized control trajectories for another $\Delta t = 30$ years (step 5), the historical effective baseline emissions must now be revised upwards by 2 ppm/year on average (Figure 5d, inset). With existing policies, the increased historical emissions would result in a 0.13°C overshoot of the $T^* = 2^\circ\text{C}$ degree goal. The most cost-effective

adjustment to existing control policies that is consistent with the temperature goal is to increase mitigation, CDR, and SRM efforts by an additional $\Delta M = 3\%$, $\Delta R = 2\%$, and $\Delta G = 2\%$ (Figure 5d), at a net-present cost of 10 trillion USD.

Scenario 2: revealed bias in projected geoeengineering (CDR and SRM) costs. Suppose that at a re-evaluation in 2050, CDR is found to be 50% more expensive than projected. The climate policy-maker directs deployment of the most cost-effective control trajectories which keep warming below $T^* = 2^\circ\text{C}$, which are re-optimized with the revised cost of CDR. The result is to decrease CDR by $\Delta R = -5\%$ and instead increase adaptation by $\Delta A = 5\%$ (Figure 5e). The shift away from expensive CDR towards adaptation results in 11.5 trillion USD of avoided net present costs of control deployments, with little difference in climate damage outcomes.

Suppose that after an additional 30 years, during which SRM is ramped up to a modest but non-zero level $G = 5\%$ (Figure 4a), it becomes clear that the costs of unintended side-effect damages of SRM are less than half as large as expected. In this scenario, the optimal future trajectory is to expand SRM deployments in the 22nd Century to $G \approx 20\%$ (resulting in $\Delta T_G = T_{M,R,G} - T_{M,R} \approx -1.0^\circ\text{C}$ of cooling, up from -0.6°C ; Figure 5f, inset) and reduce future mitigation levels by $\Delta M = -10\%$ (Figure 5f), resulting in another 12.6 trillion USD of avoided net present control costs.

Scenario 3: revealed bias in estimates of climate sensitivity. Suppose that by 2050, a dramatically improved suite of general circulation climate models robustly exhibits Equilibrium Climate Sensitivities of $ECS = 3.5^\circ\text{C}$, up from 3°C in recent years (55), and further improvements result in $ECS = 4^\circ\text{C}$

by 2080. Each of these revisions effectively shrinks the remaining cumulative carbon budget and thus requires sequentially increased deployments of mitigation, CDR, and SRM in order to keep warming below $T^* = 2^\circ\text{C}$ (Figures 5g, h).

This responsive policy process only works if adjustments are made sufficiently frequently. If the policy decision-maker had waited from 2020 until 2100 before re-adjusting their course for a higher climate sensitivity of $ECs = 4^\circ\text{C}$, there would already be enough warming baked into the system that $T_{M,R,G,A} = 2.2^\circ\text{C} > T^*$ of warming would be inevitable—even if the optimal policy from 2020 (Figure 4a,b) had been perfectly implemented.

Discussion

Few studies have considered the combined use of mitigation, carbon dioxide removal (CDR), solar radiation modification (SRM), and adaptation for controlling climate damages. We have developed a multi-control, time-dependent model of optimally cost-beneficial or cost-effective climate policies, which extends and improves upon previous work (4). Another recent study (5) uses a similar conceptual model with time-dependent controls to analytically investigate the differences between different climate controls; however, this model's climate physics are reduced to a simple empirical relationship that is not as clearly applicable to the case of significant SRM, where the direct link between cumulative emissions and temperature falls apart. Despite these differences, our study reproduces two key conceptual results of both earlier studies: 1) the four different climate controls are not interchangeable, as they enter at different stages of the causal chain between emissions and damages, and 2) the most cost-effective solution to limiting climate damages is to use all four controls at our disposal. The first result emerges from the role of each control in modifying the basic stock-flow properties of the carbon and heat budgets in the climate system. The second result is a direct consequence of marginal control costs which 1) begin at zero and 2) are concave, and is not guaranteed to hold if either assumption fails. For example, if learning effects are strong enough to cause fractional deployment costs to become convex, then a single-control strategy could be more appealing. Alternatively, if substantial R&D investments are necessary before a control is deployed, the large up-front marginal cost may be disqualifying.

We have proposed a policy response process which highlights the iterative nature of climate policy decision-making. We show that this process can be used to periodically correct for revealed biases in our understanding of the climate-economic system, in order to avoid unanticipated climate damages or "excessive" spending on climate controls. We view our proposed policy response process as an improvement over previously proposed "sequential" and "adaptive" strategies, in which policies are periodically re-evaluated by following instructions from a subjectively-defined decision flow chart (e.g. 56). In our process, policy re-evaluations are always optimally cost-beneficial or cost-effective, although the parameters that govern this optimization can be periodically re-adjusted. We argue that our policy process based on re-optimization is more defensible than previous approaches but retains the benefits of the process being "adaptive".

For clarity of exposition, we have presented a fully deterministic version of the MARGO model. In actuality, key

inputs such as the climate feedback parameter B (and the related climate sensitivity ECs) and the damage function $D(T)$ are extremely uncertain. Propagation of these uncertainties through a convex damage function typically increases expected climate damages and strengthens the case for early and aggressive climate control (57). Future work includes 1) extending MARGO to a stochastic programming approach that accounts for uncertainty in the various input parameters (see Methods) and 2) implementing a Bayesian policy response process where prior parameter distributions can be updated based on observed outcomes (58) or improved parameter estimates from research developments. Stochastic programming of IAMs is significantly complicated by their endogenous economic models (59); the model presented here is significantly more endogenous and may prove to be a useful framework for straight-forward multi-stage stochastic programming (60).

The greatest caveat of the present study may be the assumption of a single trusted decision-maker. This device evidently avoids the complexities of a realistic decision making process that involve multiple stake holders with conflicting interests. The costs and benefits defined here are globally-aggregated; asymmetric costs and benefits between different regions lead to diverging incentives, which are further complicated as the number of unique climate controls increases. Asymmetric multi-control incentives can be counter-intuitive: for example, one study suggests that high asymmetry in SRM damages drives even higher levels of mitigation because of the risk of SRM "free-drivers" (61).

Even in the case where climate control policies are prescribed by a single hypothetical decision-maker, there are sure to be inefficiencies in their implementation which we argue are more likely to result in under-deployment of controls than over-deployment. Considerable caution must be taken whenever relying on substantial CDR or SRM since neither of these controls exist as socio-technological systems capable of influencing climate, resulting in a "moral hazard" that shifts the burden to unconsenting future generations (25, 62).

The MARGO model is an idealized model which highlights the qualitatively different roles of mitigation, CDR, adaptation, and SRM in climate control. Both economic and physical components of the model have been abstracted as much as possible to highlight a small number ($N \approx 9$) of key parameters that govern the leading order behavior of the system (as compared to widely-used IAMs: 26, 63, 64): the climate feedback parameter B (related to the equilibrium climate sensitivity $ECs = F_{2 \times CO_2}$), the ocean heat uptake rate κ , the exogenous economic growth rate γ , the discount rate ρ , the climate damage parameter β , and the controls costs C_M, C_R, C_A, C_G (SI Text 2 and Table S1). We show how the model can be used to investigate the sensitivity of "optimal" climate control policies to poorly constrained parameters, such as future control costs, and value-dependent parameters, such as the discount rate. We believe that our model resides in a sweet spot of being more realistic than semi-analytic models and easier to understand than conventional IAMs. We demonstrate that our model can be easily modified to reproduce the qualitative results of other studies (e.g. 6, 65, SI Text 3) and hope that it will be a useful community tool for extending simpler models, interpreting more comprehensive models, and bridging the gaps between climate economists, scientists, policy decision-makers, and the public (66–68).

578 Materials and Methods

579 All data and figures used in the study can be found at github.com/hdrake/OptimizeClimate and are readily reproduced or modified by
580 the Jupyter notebooks therein.
581

582 **Control costs.** The scaling costs for the four controls used in the
583 present study are subjectively tuned; we here describe our rationale
584 for choosing the parameter values. We remind the reader that the
585 purpose of the MARGO model is to reveal insights about trade
586 offs between the multiple controls and the dependence of model
587 results on structural and parameteric choices. The interested reader
588 can choose their own parameter values and see how the results
589 change by visiting our web-browser application at github.com/hdrake/OptimizeClimate (placeholder until we have a better webapp).
590

591 The costs of mitigation are set according to the Working Group
592 III contribution to Intergovernmental Panel on Climate Change's
593 Fifth Assessment Report (69). In aggressive mitigation scenarios
594 where CO_{2e} emissions decrease 78% to 118% by 2100, they estimate
595 abatement costs of about 2% of GWP (see their Figure 6.21, panel f).
596 Thus, we set the scaling cost of mitigation controls to $C_M = \bar{C}_M E(t)$,
597 where the cost of mitigating all emissions is $\bar{C}_M = 2\%$ of the GWP
598 $E(t)$.

599 The costs of CDR are set according to bottom-up cost estimates
600 from (36, their Table 2). We compute the mean cost of negative-
601 emissions technologies, where we weight the median cost of each
602 negative-emissions technology (in USD/tCO₂) by its upper-bound
603 potential for carbon-dioxide removal (in GtCO₂/year). This leads
604 to a total potential of roughly $q_0/2 \approx 26$ GtCO₂/year at an average
605 cost of $\bar{C}_R = 110$ USD/tCO₂. The scaling cost is thus set based
606 on an estimate for $R = 50\%$, i.e. $C_R (\frac{1}{2})^2 = \bar{C}_R q_0/2$ or $C_R =$
607 $2\bar{C}_R q_0 = 13$ trillion USD/year.

608 The costs of SRM largely reflect the costs of unintended climate
609 damages that result due to their imperfect compensation for GHG
610 forcing (70). Relative to both the costs of unintended damages
611 and the costs of other climate controls, the direct costs of SRM
612 measures are thought to be small (19), as in the most commonly
613 studied proposal of releasing gaseous sulfate aerosol precursors into
614 the stratosphere to reflect sunlight back to space. The reference cost
615 of SRM is thus given by $C_G(t) = \bar{C}_G E(t)$, where \bar{C}_G is the damage
616 due to deploying $-F_\infty \equiv -F(t \rightarrow \infty) = -8.5$ Wm⁻² worth of SRM,
617 as a fraction of the exogenous GWP $E(t)$. In the face of considerable
618 uncertainties about the climate impacts of large-scale SRM (70), we
619 make the conservative assumption that the unintended damages of
620 SRM are as large as the uncontrolled damages due to an equivalent
621 amount of CO_{2e} forcing (as in 6, 71), i.e. $\bar{C}_G \equiv \beta(F_\infty/B)^2 \approx 4.6\%$,
622 where F_∞/B is the equilibrium temperature response to a fixed
623 radiative forcing of $F_\infty = 8.5$ Wm⁻².

624 The costs of adaptation are estimated based on a recent joint
625 report from the United Nations, the Bill and Melinda Gates Founda-
626 tion, and the World Bank. They estimate that adaptation measures
627 costing 1.8 trillion USD from 2020 to 2030 generate more than
628 five times as much in total net benefits. Here, we make the crude
629 assumption that this level of spending (180 billion USD / year)
630 reduces climate damages by $A = 20\%$, i.e. $C_A (\frac{1}{5})^2 = 180$ billion
631 USD / year, or $C_A = 4.5$ trillion USD / year. We additionally cap
632 adaptation at $A < 1/2$, recognizing that adaptation to all climate
633 impacts is impossible: there will always be residual damages that
634 can not be adapted to (20).

635 **Optimization method.** We use the Interior Point Optimizer (72)
636 (<https://github.com/coin-or/lpopt>), an open source software package for
637 large-scale nonlinear optimization, to minimize objective functions
638 representing benefits and costs to society subject to assumed policy
639 constraints. In practice, the control variables $\alpha \in \mathcal{A} = \{M, R, G, A\}$
640 are discretized into $N = (t_f - t_0)/\delta t$ timesteps (default $\delta t = 5$ years,
641 $N = 36$) resulting in a $4N$ -dimensional optimization problem. In the
642 default (deterministic and convex) configuration, the model takes
643 only $\mathcal{O}(10$ ms) to solve after just-in-time compiling and effectively
644 provides user feedback in real time. This makes the model amenable
645 to our forthcoming interactive web application, which is inspired by
646 the impactful En-ROADS model web application (73).

647 The model was designed from the beginning with the goal of
648 eventual use in stochastic simulations where 1) the deterministic

649 scalar objective function can be generalized to an expected value of
650 a probabilistic ensemble of simulations that sample an uncertain
651 parameter space, and 2) deterministic constraints can be generalized
652 to probabilistic constraints (e.g. having a two-thirds chance of
653 keeping temperatures below a goal T^*), although these features are
654 still under active development.

655 **Social, technological, and economic inertia.** For each control $\alpha \in$
656 $\mathcal{A} = \{M, R, G, A\}$, we assert a maximum deployment rate

$$\left| \frac{d\alpha}{dt} \right| \leq \dot{\alpha}, \quad [14] \quad 657$$

658 as a crude parameterization of social, technological, and economic
659 inertia (74), which acts to forbid implausibly aggressive deployment
660 (75) and phase-out scenarios (see SI Text 2 for more discussion).
661 We set $\dot{M} \equiv \dot{R} \equiv 1/40$ years⁻¹ in line with the most ambitious
662 climate goals (2) and $\dot{G} = 1/20$ years⁻¹ to reflect the technological
663 simplicity of attaining a large SRM forcing relative to mitigation
664 and CDR. We interpret adaptation deployment costs as buying
665 insurance against future damages at a fixed annual rate $C_A A^2$, with
666 $\dot{A} = 0$, which can be increased or decreased upon re-evaluation at a
667 later date.

668 We also set a control readiness condition which optionally limits
669 how soon each control is "ready" to be deployed. In particular, in
670 the default configuration we set $t_R = 2030$ and $t_G = 2050$ because
671 CDR has not yet been deployed at a climatically significant scale
672 (76) and SRM does not yet exist as a socio-technological system
673 (25).

674 **Two-box energy balance model.** The evolution of the global-mean
675 near-surface temperature anomaly (relative to the initial time $t_0 =$
676 2020) is determined by the two-box linear energy balance model
677 (77):

$$C_U \frac{dT}{dt} = -BT - \kappa(T - T_D) + F(t), \quad [15]$$

$$C_D \frac{dT_D}{dt} = \kappa(T - T_D), \quad [16]$$

678 where eq. 15 represents the upper ocean with average temperature
679 anomaly T , and eq. 16 represents the deep ocean with an average
680 temperature T_D . The near-surface atmosphere exchanges heat
681 rapidly with the upper ocean and thus the global-mean near-surface
682 air temperature is also given by T . The physical model parameters
683 are: the upper ocean heat capacity $C_U = 7.3$ W yr m⁻² K⁻¹ (in-
684 cluding a negligible contribution $C_A \ll C_U$ from the atmosphere);
685 the deep ocean heat capacity $C_D = 106$ W yr m⁻² K⁻¹; the climate
686 feedback parameter $B = 1.13$ W m⁻² K⁻¹; and the ocean mixing
687 rate $\kappa = 0.73$ W m⁻² K⁻¹. The parameter values are taken from
688 the multi-model mean of values diagnosed from 16 CMIP5 models
689 (55). The radiative forcing and temperature anomalies at $t_0 = 2020$
690 relative to preindustrial are $F(t_0) - F(t_{\text{pre}}) = 2.5$ W m⁻² and
691 $T_0 \equiv T(t_0) - T(t_{\text{pre}}) = 1.1$ K, where we set $F_0 \equiv F(t_0) = 0$ W m⁻²
692 and $T(t_{\text{pre}}) = 0$ K for convenience.

693 Since, by construction, the anthropogenic forcing $F(t)$ varies on
694 timescales longer than the fast relaxation timescale $\tau_U = C_U/(B +$
695 $\kappa) = 4$ years, we can ignore the time-dependence in the upper ocean
696 and approximate

$$T \approx \frac{F + \kappa T_D}{B + \kappa}, \quad [17] \quad 693$$

694 where the evolution of the deep ocean

$$C_D \frac{dT_D}{dt} \approx -\frac{B\kappa}{B + \kappa} T_D + \frac{\kappa}{B + \kappa} F \quad [18] \quad 695$$

696 occurs on a slower timescale $\tau_D \equiv \frac{C_D}{B} \frac{B + \kappa}{\kappa} = 240$ years (77).

697 This approximation is convenient because it permits a simple closed
698 form solution, but should be avoided if the model is applied to
699 scenarios with rapidly changing forcing, such as studies of the tran-
700 sient response to an instantaneous doubling of CO₂ or the SRM
701 "termination effect" (see SI Text 1 for validation of the approxima-
702 tion). Plugging the exact solution to eq. 18 into eq. 17 gives the
703 closed-form solution

$$T(t) - T_0 = \frac{F(t)}{B + \kappa} + \frac{\kappa}{B} \frac{1}{(B + \kappa)} \int_{t_0}^t \frac{e^{-(t-t')/\tau_D}}{\tau_D} F(t') dt'. \quad [19] \quad 704$$

705 The evolution of the controlled temperature anomaly (eq. 5; Figure
706 2c) has the same form but is instead driven by the controlled net
707 radiative forcing $F_{M,R,G}$.

708 We identify the first term on the right hand side of eq. 19 and
709 eq. 5 as the transient climate response (78), which dominates for
710 $t - t_0 \ll \tau_D$, while the second term is a slower "recalcitrant" response
711 due to a weakening of ocean heat uptake as the deep ocean comes
712 to equilibrium with the upper ocean (77). While the contribution
713 of the recalcitrant component to historical warming is thought to
714 be small, it contributes significantly to 21st century and future
715 warming (77, 78).

716 The behavior of the model on short and long timescales is illus-
717 trated by applying it to the canonical climate change experiment in
718 which CO₂ concentrations increase at 1% per year until doubling.
719 The temperature anomaly first rapidly increases until it reaches the
720 Transient Climate Sensitivity $TCS = \frac{F_{2\times}}{B + \kappa} = 1.9^\circ\text{C}$ around the
721 time of doubling $t = t_{2\times}$, with $t_{2\times} - t_0 \ll \tau_D$ and $F_{2\times} = \alpha \ln(2)$,
722 and then gradually asymptotes to the Equilibrium Climate Sensi-
723 tivity $ECS = \frac{F_{2\times}}{B} = 3.1^\circ\text{C} > TCS$ on a much longer timescale
724 $t - t_0 \gg \tau_D$.

725 **Model validation.** In Section 1 of the SI, we show that subjecting the
726 MARGO energy balance model to a stylized RCP8.5-like forcing
727 accurately reproduces the multi-model mean response from an
728 ensemble of 35 comprehensive general circulation climate models
729 from the CMIP5 ensemble (Figure S2). In SI Text 3, we show that
730 by tweaking just a few of these default parameter values (SI Tables 1
731 and 2), the model replicates the qualitative results of studies ranging
732 from analytical control theory analysis of SRM deployments (65) to
733 numerical optimizations of mitigation, CDR, and SRM deployments
734 in a recent application of DICE (6), a commonly used Integrated
735 Assessment Model (26).

736 **ACKNOWLEDGMENTS.** This material is based upon work sup-
737 ported by the National Science Foundation Graduate Research
738 Fellowship Program under Grant No. 174530. Any opinions, find-
739 ings, and conclusions or recommendations expressed in this material
740 are those of the author(s) and do not necessarily reflect the views
741 of the National Science Foundation.

742 1. GP Peters, et al., Carbon dioxide emissions continue to grow amidst slowly emerging climate
743 policies. *Nat. Clim. Chang.* **10**, 3–6 (2020) Number: 1 Publisher: Nature Publishing Group.
744 2. Intergovernmental Panel on Climate Change, *Global warming of 1.5°C*. (2018) OCLC:
745 1056192590.
746 3. EA Parson, Opinion: Climate policymakers and assessments must get serious about climate
747 engineering. *Proc. Natl. Acad. Sci.* **114**, 9227–9230 (2017) Publisher: National Academy of
748 Sciences Section: Opinion.
749 4. JM Deutch, Joint allocation of climate control mechanisms is the cheapest way to reduce
750 global climate damage. *MIT Cent. for Energy Environ. Policy Res. Work. Pap. Ser.* (2019).
751 5. J Moreno-Cruz, G Wagner, D Keith, An Economic Anatomy of Optimal Climate Policy, (Social
752 Science Research Network, Rochester, NY), SSRN Scholarly Paper ID 3001221 (2018).
753 6. M Beliaia, Optimal Climate Strategy with Mitigation, Carbon Removal, and Solar Geoen-
754 gineering. *arXiv:1903.02043 [econ, q-fin]* (2019) arXiv: 1903.02043.
755 7. JR Lamontagne, PM Reed, G Marangoni, K Keller, GG Garner, Robust abatement pathways
756 to tolerable climate futures require immediate global action. *Nat. Clim. Chang.* **9**, 290–294
757 (2019) Number: 4 Publisher: Nature Publishing Group.
758 8. EA Parson, DW Keith, End the Deadlock on Governance of Geoengineering Research. *Sci-*
759 *ence* **339**, 1278–1279 (2013) Publisher: American Association for the Advancement of Sci-
760 ence Section: Policy Forum.
761 9. S Schäfer, et al., Field tests of solar climate engineering. *Nat. Clim. Chang.* **3**, 766–766
762 (2013) Number: 9 Publisher: Nature Publishing Group.
763 10. K Caldeira, KL Ricke, Prudence on solar climate engineering. *Nat. Clim. Chang.* **3**, 941–941
764 (2013) Number: 11 Publisher: Nature Publishing Group.
765 11. W Steffen, et al., Trajectories of the Earth System in the Anthropocene. *Proc. Natl. Acad. Sci.*
766 *United States Am.* **115**, 8252–8259 (2018).
767 12. S Manabe, RT Wetherald, Thermal equilibrium of the atmosphere with a given distribution of
768 relative humidity. *J. Atmospheric Sci.* **24**, 241–259 (1967).
769 13. R Revelle, W Broecker, H Craig, C Kneeling, J Smagorinsky, Restoring the quality of our
770 environment: report of the environmental pollution panel. Atmospheric carbon dioxide. *Pres-*
771 *ident's Science Advisory Committee, United States, US Government Printing Office: Wash-*
772 *ington, DC* (1965).
773 14. WW Kellogg, SH Schneider, Climate Stabilization: For Better or for Worse? *Science* **186**,
774 1163–1172 (1974) Publisher: American Association for the Advancement of Science Section:
775 Articles.
776 15. NR Council, et al., Policy implications of greenhouse warming in *Report of the Committee*
777 *on Science, Engineering and Public Policy*. (National Academy Press Washington, DC), p.
778 127 (1991).

779 16. PJ Crutzen, Albedo Enhancement by Stratospheric Sulfur Injections: A Contribution to Re-
780 solve a Policy Dilemma? *Clim. Chang.* **77**, 211 (2006).
781 17. DG Victor, MG Morgan, F Apt, J Steinbruner, The Geoengineering Option - A Last Resort
782 against Global Warming Essay. *Foreign Aff.* **88**, 64–76 (2009).
783 18. HJ Buck, Geoengineering: Re-making Climate for Profit or Humanitarian Intervention? *Dev.*
784 *Chang.* **43**, 253–270 (2012) _eprint: <https://onlinelibrary.wiley.com/doi/pdf/10.1111/j.1467-7660.2011.01744.x>.
785 19. J McClellan, DW Keith, J Apt, Cost analysis of stratospheric albedo modification delivery
786 systems. *Environ. Res. Lett.* **7**, 034019 (2012) Publisher: IOP Publishing.
787 20. K Dow, et al., Limits to adaptation. *Nat. Clim. Chang.* **3**, 305–307 (2013) Number: 4 Publisher:
788 Nature Publishing Group.
789 21. JA Flegal, A Gupta, Evoking equity as a rationale for solar geoengineering research? Scruti-
790 nizing emerging expert visions of equity. *Int. Environ. Agreements: Polit. Law Econ.* **18**,
791 45–61 (2018).
792 22. B Haerlin, D Parr, How to restore public trust in science. *Nature* **400**, 499–499 (1999) Number:
793 6744 Publisher: Nature Publishing Group.
794 23. J Lacey, M Howden, C Civanovic, RM Colvin, Understanding and managing trust at the
795 climate science-policy interface. *Nat. Clim. Chang.* **8**, 22–28 (2018) Number: 1 Publisher:
796 Nature Publishing Group.
797 24. KL Ricke, JB Moreno-Cruz, K Caldeira, Strategic incentives for climate geoengineering coalitions
798 to exclude broad participation. *Environ. Res. Lett.* **8**, 014021 (2013) Publisher: IOP
799 Publishing.
800 25. JA Flegal, AM Hubert, DR Morrow, JB Moreno-Cruz, Solar Geoengineering: Social Science,
801 Legal, Ethical, and Economic Frameworks. *Annu. Rev. Environ. Resour.* **44**, 399–423 (2019)
802 _eprint: <https://doi.org/10.1146/annurev-environ-102017-030032>.
803 26. WD Nordhaus, An Optimal Transition Path for Controlling Greenhouse Gases. *Science* **258**,
804 1315–1319 (1992) Publisher: American Association for the Advancement of Science Section:
805 Articles.
806 27. G Luderer, et al., Economic mitigation challenges: how further delay closes the door for
807 achieving climate targets. *Environ. Res. Lett.* **8**, 034033 (2013) Publisher: IOP Publishing.
808 28. United Nations Framework Convention on Climate Change, Paris agreement. Article 2(a)
809 (<https://unfccc.int/process-and-meetings/the-paris-agreement/the-paris-agreement>) (2015).
810 29. J Rogelj, et al., Paris Agreement climate proposals need a boost to keep warming well below
811 2°C. *Nature* **534**, 631–639 (2016) Number: 7609 Publisher: Nature Publishing Group.
812 30. J Weyant, Some Contributions of Integrated Assessment Models of Global Climate Change.
813 *Rev. Environ. Econ. Policy* **11**, 115–137 (2017) Publisher: Oxford Academic.
814 31. J Bezanson, A Edelman, S Karpinski, V Shah, Julia: A Fresh Approach to Numerical Com-
815 puting. *SIAM Rev.* **59**, 65–98 (2017).
816 32. W Nordhaus, P Sator, Dice 2013r: Introduction and user's manual. *Yale Univ. Natl. Bureau*
817 *Econ. Res. USA* (2013).
818 33. K Riahi, et al., The Shared Socioeconomic Pathways and their energy, land use, and green-
819 house gas emissions implications: An overview. *Glob. Environ. Chang.* **42**, 153–168 (2017).
820 34. S Solomon, GK Plattner, R Knutti, P Friedlingstein, Irreversible climate change due to car-
821 bon dioxide emissions. *Proc. Natl. Acad. Sci.* **106**, 1704–1709 (2009) Publisher: National
822 Academy of Sciences Section: Physical Sciences.
823 35. DP Marshall, L Zanna, A Conceptual Model of Ocean Heat Uptake under Climate Change. *J.*
824 *Clim.* **27**, 8444–8465 (2014) Publisher: American Meteorological Society.
825 36. S Fuss, et al., Negative emissions—Part 2: Costs, potentials and side effects. *Environ. Res.*
826 *Lett.* **13**, 063002 (2018) Publisher: IOP Publishing.
827 37. M Lickley, BB Cael, S Solomon, Time of Steady Climate
828 Change. *Geophys. Res. Lett.* **46**, 5445–5451 (2019) _eprint:
829 <https://agupubs.onlinelibrary.wiley.com/doi/pdf/10.1029/2018GL081704>.
830 38. HD Matthews, K Caldeira, Stabilizing climate requires near-
831 zero emissions. *Geophys. Res. Lett.* **35** (2008) _eprint:
832 <https://agupubs.onlinelibrary.wiley.com/doi/pdf/10.1029/2007GL032388>.
833 39. MJ Glotter, RT Pierrehumbert, JW Elliott, NJ Matteson, EJ Moyer, A simple carbon cycle
834 representation for economic and policy analyses. *Clim. Chang.* **126**, 319–335 (2014).
835 40. P Christensen, K Gillingham, W Nordhaus, Uncertainty in forecasts of long-run economic
836 growth. *Proc. Natl. Acad. Sci.* **115**, 5409–5414 (2018).
837 41. C Azar, SH Schneider, Are the economic costs of stabilising the atmosphere prohibitive?
838 *Ecol. Econ.* **42**, 73–80 (2002).
839 42. N Gnanemang, SN Willner, A Levermann, Paris Climate Agreement passes the cost-benefit
840 test. *Nat. Commun.* **11**, 1–11 (2020) Number: 1 Publisher: Nature Publishing Group.
841 43. FP Ramsey, A Mathematical Theory of Saving. *The Econ. J.* **38**, 543–559 (1928) Publisher:
842 [Royal Economic Society, Wiley].
843 44. RM Solow, The Economics of Resources or the Resources of Economics. *The Am. Econ.*
844 *Rev.* **64**, 1–14 (1974) Publisher: American Economic Association.
845 45. N Stern, NH Stern, GB Treasury, *The Economics of Climate Change: The Stern Review*.
846 (Cambridge University Press), (2007).
847 46. K Arrow, et al., Determining Benefits and Costs for Future Generations. *Science* **341**, 349–
848 350 (2013) Publisher: American Association for the Advancement of Science Section: Policy
849 Forum.
850 47. SH Schneider, The Greenhouse Effect: Science and Policy. *Science* **243**, 771–781 (1989)
851 Publisher: American Association for the Advancement of Science Section: Articles.
852 48. RSJ Tol, Is the Uncertainty about Climate Change too Large for Expected Cost-Benefit Anal-
853 ysis? *Clim. Chang.* **56**, 265–289 (2003).
854 49. J Koomey, Moving beyond benefit-cost analysis of climate change. *Environ. Res. Lett.* **8**,
855 041005 (2013) Publisher: IOP Publishing.
856 50. RB Alley, et al., Abrupt Climate Change. *Science* **299**, 2005–2010 (2003).
857 51. M Burke, SM Hsiang, E Miguel, Global non-linear effect of temperature on economic produc-
858 tion. *Nature* **527**, 235–239 (2015) Number: 7577 Publisher: Nature Publishing Group.
859 52. JK Hammitt, Evaluation Endpoints and Climate Policy: Atmospheric Stabilization, Benefit-
860 Cost Analysis, and Near-Term Greenhouse-Gas Emissions. *Clim. Chang.* **41**, 447–468
861 (1999).
862

- 863 53. JP Weyant, A Critique of the Stern Review's Mitigation Cost Analyses and Integrated Assess-
864 ment. *Rev. Environ. Econ. Policy* 2, 77–93 (2008) Publisher: Oxford Academic.
- 865 54. R Millar, M Allen, J Rogelj, P Friedlingstein, The cumulative carbon budget and its implications.
866 *Oxf. Rev. Econ. Policy* 32, 323–342 (2016) Publisher: Oxford Academic.
- 867 55. O Geoffroy, et al., Transient Climate Response in a Two-Layer Energy-Balance Model. Part
868 I: Analytical Solution and Parameter Calibration Using CMIP5 AOGCM Experiments. *J. Clim.*
869 26, 1841–1857 (2012) Publisher: American Meteorological Society.
- 870 56. RJ Lempert, ME Schlesinger, SC Bankes, When we don't know the costs or the benefits:
871 Adaptive strategies for abating climate change. *Clim. Chang.* 33, 235–274 (1996).
- 872 57. G Wagner, RJ Zeckhauser, Confronting Deep and Persistent Climate Uncertainty, (Social
873 Science Research Network, Rochester, NY), SSRN Scholarly Paper ID 2818035 (2016).
- 874 58. S Shayegh, VM Thomas, Adaptive stochastic integrated assessment modeling of optimal
875 greenhouse gas emission reductions. *Clim. Chang.* 128, 1–15 (2015).
- 876 59. B Crost, CP Traeger, Optimal climate policy: Uncertainty versus Monte Carlo. *Econ. Lett.*
877 120, 552–558 (2013).
- 878 60. M Webster, N Santen, P Parpas, An approximate dynamic programming framework for mod-
879 eling global climate policy under decision-dependent uncertainty. *Comput. Manag. Sci.* 9,
880 339–362 (2012).
- 881 61. JB Moreno-Cruz, Mitigation and the geoengineering threat. *Resour. Energy Econ.* 41, 248–
882 263 (2015).
- 883 62. S Fuss, et al., Betting on negative emissions. *Nat. Clim. Chang.* 4, 850–853 (2014) Number:
884 10 Publisher: Nature Publishing Group.
- 885 63. RS Tol, On the optimal control of carbon dioxide emissions: an application of FUND. *Environ.*
886 *Model. & Assess.* 2, 151–163 (1997).
- 887 64. C Hope, The marginal impact of CO₂ from page2002: an integrated assessment model incor-
888 porating the IPCC's five reasons for concern. *Integr. assessment* 6 (2006).
- 889 65. SA Soldatenko, RM Yusupov, Optimal Control of Aerosol Emissions into the Stratosphere to
890 Stabilize the Earth's Climate. *Izvestiya, Atmospheric Ocean. Phys.* 54, 480–486 (2018).
- 891 66. SH Schneider, Integrated assessment modeling of global climate change: Transparent rational
892 tool for policy making or opaque screen hiding value-laden assumptions? *Environ. Model.*
893 *& Assess.* 2, 229–249 (1997).
- 894 67. RS Pindyck, The Use and Misuse of Models for Climate Policy. *Rev. Environ. Econ. Policy*
895 11, 100–114 (2017) Publisher: Oxford Academic.
- 896 68. HJ Buck, What can geoengineering do for us? public participation and the new media land-
897 scape in *Paper for workshop: The ethics of solar radiation management, 18 Oct 2010, Uni-*
898 *versity of Montana.* (2010).
- 899 69. LE Clarke, et al., Assessing Transformation Pathways. In: Climate Change 2014: Mitigation
900 of Climate Change. Contribution of Working Group III to the Fifth Assessment Report of the
901 Intergovernmental Panel on Climate Change, Technical report (2014).
- 902 70. PJ Irvine, et al., Towards a comprehensive climate impacts assess-
903 ment of solar geoengineering. *Earth's Futur.* 5, 93–106 (2017) _eprint:
904 <https://agupubs.onlinelibrary.wiley.com/doi/pdf/10.1002/2016EF000389>.
- 905 71. M Goes, N Tuana, K Keller, The economics (or lack thereof) of aerosol geoengineering. *Clim.*
906 *Chang.* 109, 719–744 (2011).
- 907 72. A Wächter, LT Biegler, On the implementation of an interior-point filter line-search algorithm
908 for large-scale nonlinear programming. *Math. Program.* 106, 25–57 (2006).
- 909 73. LS Siegel, et al., En-roads simulator reference guide, (Technical Report), Technical report
910 (2018).
- 911 74. M Ha-Duong, MJ Grubb, JC Hourcade, Influence of socioeconomic inertia and uncertainty on
912 optimal CO₂-emission abatement. *Nature* 390, 270–273 (1997) Number: 6657 Publisher:
913 Nature Publishing Group.
- 914 75. HJ Buck, Rapid scale-up of negative emissions technologies: social barriers and social impli-
915 cations. *Clim. Chang.* 139, 155–167 (2016).
- 916 76. JC Minx, et al., Negative emissions—Part 1: Research landscape and synthesis. *Environ.*
917 *Res. Lett.* 13, 063001 (2018) Publisher: IOP Publishing.
- 918 77. IM Held, et al., Probing the Fast and Slow Components of Global Warming by Returning
919 Abruptly to Preindustrial Forcing. *J. Clim.* 23, 2418–2427 (2010).
- 920 78. JM Gregory, PM Forster, Transient climate response estimated from radiative forcing and
921 observed temperature change. *J. Geophys. Res. Atmospheres* 113 (2008).

1

2 **Supplementary Information for**

3 **A multi-control climate policy process for a trusted decision maker**

4 **Henri F. Drake, Ronald L. Rivest, Alan Edelman, and John Deutch**

5 **Corresponding Author: Ronald L. Rivest.**

6 **E-mail: rivest@mit.edu**

7 **This PDF file includes:**

8 Supplementary text

9 Figs. S1 to S5

10 Tables S1 to S2

11 SI References

12 Supporting Information Text

13 Figure S1 shows the same information as Figure 2 of the main text, but for the cost-benefit analysis rather than the
14 cost-effectiveness analysis.

15 1. Validation of MARGO’s approximate two-box Energy Balance Model

16 **A. Comparison with CMIP5 simulations under RCP8.5.** The two-box Energy Balance Model (EBM) used in the MARGO
17 model is described in the main text Methods. Here, we validate the MARGO-EBM by comparing it to an ensemble of 35
18 CMIP5 models under the RCP8.5 forcing scenario. We further validate the MARGO-EBM’s approximation to the two-layer box
19 model (in the equilibrated-thermocline limit $C_U \ll C_D$). We validate the approximation in three different high-forcing regimes:
20 1) the RCP8.5 scenario with large but gradual changes in forcing over the 21st Century; 2) the long-term (800 year) approach
21 to equilibrium in an extended RCP8.5 scenario (ECP8.5); and 3) the short-term response to deployment and termination of
22 large-amplitude solar radiation modification (SRM).

23 First, we construct an idealized forcing scenario that is meant to approximate RCP8.5 (1) and its extension beyond 2100,
24 ECP8.5 (2). In our scenario, baseline CO_{2e} emissions: 1) increase exponentially with a growth rate of $1/37 \text{ years}^{-1}$ to reach a
25 maximum of $410 \text{ GtCO}_{2e}/\text{year}$ in 2100, approximately 7 times present-day emissions; 2) plateau between 2100 and 2120; and 3)
26 decrease linearly to zero between 2120 and 2200 (Figure S2a). As a result, CO_{2e} concentrations increase exponentially from
27 the preindustrial value $c_0 = 280 \text{ ppm}$ in 1850 to 1400 ppm in 2100. In the extended scenario ECP8.5, CO_{2e} concentrations
28 continue to grow until stabilizing at 3000 ppm in 2200* (Figure S2b). These increases in CO_{2e} drive a radiative forcing which
29 increases to $F = 8.5 \text{ W/m}^2$ by 2100 and stabilizes at $F = 12 \text{ W/m}^2$ by 2200 (Figure S2c). The forcing timeseries constructed
30 here approximates the RCP8.5 and ECP8.5 scenarios reasonably well— compare our Figure S2c with Figure 4 of Meinshausen
31 et al (2011; 2).

32 When subjecting the MARGO-EBM to the RCP8.5-like scenario introduced above, we almost exactly recover the multi-
33 model-mean warming from the CMIP5 ensemble under RCP8.5 (Figure S2d, solid black and blue lines). The excellent agreement
34 is not surprising, given that we have tuned our MARGO-EBM with parameter values calibrated to the CMIP5 models (3).
35 The climate physics-based calibration used here (3) is more realistic than the calibrations of commonly-used IAMs (4) and
36 more robust to out-of-sample climate forcings.

37 **B. Evaluation of the equilibrated-thermocline approximation.** The MARGO-EBM uses the equilibrated-thermocline approxi-
38 mation,

$$39 \quad T_{M,R,G}(t) - T_0 = \frac{F_{M,R,G}(t)}{B + \kappa} + \frac{\kappa}{B} \int_{t_0}^t e^{-\frac{t-t'}{\tau_D}} \frac{F_{M,R,G}(t')}{B + \kappa} dt', \quad [1]$$

which is a valid solution of the two-layer equations

$$40 \quad C_U \frac{dT}{dt} = -BT - \kappa(T - T_D) + F(t), \quad [2]$$

$$41 \quad C_D \frac{dT_D}{dt} = \kappa(T - T_D), \quad [3]$$

42 in the limit $C_U \ll C_D$. In Figure S2e we show that this approximation (dashed black line) introduces only very small errors
43 relative to the full solution under the ECP8.5 forcing scenario (solid black line). The full solution is computed numerically by
44 solving the two-layer EBM equations 2 and 3 using forward finite differences. If we dramatically reduce either the deep ocean
45 heat uptake rate κ or the deep ocean heat capacity C_D , as is customary in IAMs (4), then the model 1) equilibrates much too
46 quickly with the instantaneous forcing and 2) underestimates recalcitrant changes that occurs long after the radiative forcing is
47 stabilized (Figure S2e, dotted black line).

48 Since we are interested in the response of the MARGO-EBM to climate controls which may cause the controlled radiative
49 forcing $F_{M,R,G}$ to deviate substantially from a high-emissions baseline scenario, we here validate the MARGO-EBM’s response
50 to a short-term impulse of radiative forcing. In Figure S3, we modify the above ECP8.5 scenario by adding a Gaussian negative
51 radiative forcing anomaly due to short-term SRM. The negative forcing impulse is centered around 2075, has a magnitude of
52 $F_G = -GF(t \rightarrow \infty) = -3.4 \text{ Wm}^{-2}$ (for $G = 40\%$), and a timescale of $\sigma = 20 \text{ years}$ (Figure S3a). This negative forcing results
53 in a pronounced short-term *net cooling* between 2050-2070, followed by an extremely rapid warming from 2070 to 2080 as the
54 SRM program terminates (Figure S3b,c). A weak residual cooling of $0.1 \text{ }^\circ\text{C}$ propagates into the deep ocean and lingers for
55 centuries (Figure S3c). Despite the neglect of upper-ocean thermal inertia in the equilibrated-thermocline approximation, the
56 MARGO-EBM agrees well with the full solution of the two-box equations, the approximation lagging behind the full solution
57 by roughly $\tau_U = 5 \text{ years}$ (Figure S3c).

56 2. Comprehensive model equations and parameter values

57 In the cost-effectiveness framing, the full formulation of the problem

$$58 \quad \min \{ \text{discounted costs} \} \quad \text{subject to} \quad T_{M,R,G,A} < T^*$$

*In the original definition of the ECP8.5 scenario (2), much of these CO_{2e} increases are the result of increases in other gases such as Methane, Nitrous Oxide, and Hydrofluorocarbons.

is given, in closed form, by:

$$\min \left\{ [E_0(1 + \gamma)^{(t-t_0)} (\tilde{C}_M M^2 + \tilde{C}_G G^2) + C_R R^2 + C_A A^2] (1 + \rho)^{-(t-t_0)} \right\} \quad [4]$$

Subject to

$$\sqrt{1-A} \left[T_0 + \frac{a \ln \left(\frac{c_0 + \int_{t_0}^t r q (1-M) dt' - q_0 \int_{t_0}^t R dt'}{c_0} \right) - F_\infty G}{B + \kappa} + \frac{\kappa}{B} \int_{t_0}^t \frac{e^{-\frac{t'-t}{\tau_D}}}{\tau_D} \left\{ \frac{a \ln \left(\frac{c_0 + \int_{t_0}^{t'} r q (1-M) dt'' - q_0 \int_{t_0}^{t'} R dt''}{c_0} \right) - F_\infty G}{B + \kappa} \right\} dt' \right] < T^*, \quad [5]$$

59 where $\tau_D = \frac{C_D B + \kappa}{B \kappa}$ is a timescale specified by the physical parameter C_D . The cost-benefit equation can similarly be
60 derived based on the equations in the main text.

61 The problem is fully characterized by the 19 "free" parameters in equations 4 and 5, the default values of which are reported
62 in Table S1 (18 in the case of cost-effectiveness, which avoids the use of a poorly-constrained damage coefficient β). The 19
63 parameters are: 3 grid parameters $t_0, t_f, \delta t$; the 3 initial conditions T_0, c_0, E_0 ; the 1 carbon cycle parameter r ; the 4 physical
64 parameters a, B, κ , and C_D ; the 3 economic parameters β, ρ, γ ; and the 5 control cost parameters $C_A, C_R, \tilde{C}_M, \tilde{C}_G, F_\infty$.
65 The baseline emissions timeseries $q(t)$ is treated as exogenous and must be prescribed as an input. In the cost-effectiveness
66 framework, the poorly-constrained damage parameter β is replaced by a prescribed temperature goal T^* . The grid, initial
67 condition, and physical parameters are well constrained, while the economic and cost parameters are heuristic interpretations
68 of the wider climate and economic literature.

69 The control variables $\alpha \in \mathcal{A} = \{M, R, G, A\}$ satisfy several additional constraints, which could be thought of as an additional
70 20 parameters, at most, although many end up being unimportant or redundant across several parameters (1 and 2 are necessary
71 physical constraints on the controls whereas 3, 4, and 5 simply make the model's behavior more realistic):

- 72 1. The controls must be positive, $\alpha \geq 0$;
- 73 2. They have an upper bound: $\alpha < \alpha_{\max}$. $M_{\max} = 1$ is by set by the definition of mitigation. $G_{\max} = 1$ is chosen because it
74 results in a negative radiative forcing that exactly offsets the maximum GHG forcing of 8.5 W/m^2 . We set $A_{\max} = 40\%$
75 in acknowledgement of practical (5) and theoretical (6) limits to adaptability (this is meant as more of a symbolic
76 gesture rather than an estimate of how much climate damage might be adaptable). Finally, $R = 50\%$ is set based on a
77 recent bottom-up estimate of the potential for carbon dioxide removal of existing (but not necessarily scalable) negative
78 emissions technologies.
- 79 3. They have an initial condition $\alpha(t_0) = \alpha_0$, which are all set to zero except for $M_0 = 10\%$, since none of the other controls
80 have yet been deployed at scale.
- 81 4. We set maximum deployment and termination rates $\left| \frac{d\alpha}{dt} \right| < \dot{\alpha}$, which represent economic, technological, and social
82 inertia. We set $\dot{M} = \dot{R} = 1/40 \text{ years}^{-1}$ as an upper limit on plausible timescales of global energy transition. On the other
83 hand, we set $\dot{G} = 1/20 \text{ years}^{-1}$ to reflect the fact that solar geo-engineering deployment capacity could in principle be
84 ramped-up very quickly, possibly even in the absence of global governance or regulation. We interpret adaptation costs
85 as buying insurance against future damages up-front, with both benefits and costs spread evenly in the future. Thus, we
86 set $\dot{A} = 0$. The caveat is that we allow control policy re-evaluations, at which point the value of adaptation can in that
87 timestep be increased or decreased to a new level (see Figure 5 of main text), without a limit on the rate of increase.
- 88 5. We implement "readiness" constraints, $\alpha(t) = 0$ for all $t < t_\alpha$, to reflect the fact that some controls, such as geoengineering
89 (both carbon and solar), do not yet exist as climate-relevant socio-technological systems (7). In particular, we set
90 $t_R = 2030$ and $t_G = 2050$.

91 3. Qualitative replications of other climate control model analysis

92 To illustrative the potential utility of MARGO as a community tool, we show how run-time parameter values in MARGO can be
93 tweaked to match the model configurations and results of other studies of climate control policies. One the one hand, MARGO
94 can be tuned to the inputs and outputs of a comprehensive multi-control IAM configuration to reproduce its qualitative results
95 (Section A; 8); on the other hand, MARGO can be simplified by setting many of the parameters to zero to emulate an analytical
96 model of climate control by solar radiation modification (SRM) only (Section B; 9). The goal of this section is to show how
97 with minimal modifications to the default MARGO model, we are able to replicate key figures from two very different studies.
98 For discussion of the figures we attempt to replicate, we refer readers to the original studies (8, 9).

Parameter	Default Configuration
t_0	2020
t_f	2200
δt	5 yr
c_0	460 ppm
T_0	1.1 K
a	4.97 W m^{-2}
r	50%
B	$1.13 \text{ W m}^{-2} \text{ K}^{-1}$
κ	$0.72 \text{ W m}^{-2} \text{ K}^{-1}$
C_D	$106 \text{ W yr m}^{-2} \text{ K}^{-1}$
β	$0.22 \times 10^{12} \text{ \$ yr}^{-1} \text{ K}^{-2}$
ρ	1%
E_0	$100 \times 10^{12} \text{ \$ yr}^{-1}$
γ	2%
C_A	$4.5 \times 10^{12} \text{ \$ yr}^{-1}$
C_R	$13 \times 10^{12} \text{ \$ yr}^{-1}$
C_M	2% (of GWP)
C_G	4.6% (of GWP)
F_∞	8.5 W m^{-2}

Table S1. Values of the 19 free parameters that characterize the MARGO model.

99 **A. Belaia (2019): A multi-control extension of DICE with Mitigation, Carbon Dioxide Removal, and Solar Geo-engineering.**
100 Belaia (2019) extend DICE, a commonly-used globally-aggregated general equilibrium IAM, to include carbon dioxide removal
101 (CDR) and solar radiative modification– which they refer to as solar geoengineering (SG)– to supplement DICE’s emissions
102 mitigation in controlling climate damages (8).

103 To implement CDR and SRM, Belaia (2019) make two fundamental changes to DICE. Their modelling of SRM forcing
104 is identical to ours. In terms of costs, they similarly make the conservative assumption that SRM costs are dominated by
105 unintended side effects and scale with the damage of an equivalent amount of GHG forcing, but they include this damage cost
106 as an additive term to the climate damages rather than the control costs. Their approach is thus similar to ours in the case of
107 cost-benefit analysis, but in the cost-effectiveness case they effectively ignore indirect SRM damages while reaping the benefits
108 of its low direct costs. The version of DICE they use already permits moderate negative emissions, as an extension of the
109 emissions mitigation curve to 120%, i.e. 100% mitigation of baseline emissions mitigation plus removal of an addition 20%
110 of baseline emissions). To extend this further, Belaia (2019) allow for substantial CDR by extending the mitigation curve
111 indefinitely, although the cost curves are convex such that CDR becomes increasingly expensive. They also appear to have
112 modified the functional form of emissions mitigation to keep CDR costs relatively low. The rationale for modelling CDR as an
113 extension of mitigation is unclear, since 1) emissions mitigation and carbon dioxide removal are distinct physical, industrial,
114 and economic processes and 2) marginal CDR costs today are already lower than the backstop mitigation costs assumed in
115 their scenarios.

116 To approximate the DICE configuration used by Belaia (2019), we make the changes to MARGO’s default parameter
117 values reported in Table S2. Notably, we extended the time from 2200 to 2500, increased the reference costs for mitigation by
118 about 75%, and increased the reference costs for SRM by about 175%. We found it necessary to modify the physical climate
119 parameters in order to match their CO_{2e} concentrations, radiative forcing, and temperatures based on their baseline emissions
120 scenario $q(t)$, which we approximated with piece-wise quadratic functions (Figure S4a, blue line). Additionally, we omit
121 adaptation and carbon dioxide removal, $A_{\max} \equiv R_{\max} \equiv 0$; we effectively remove the upper limit on mitigation $M_{\max} = 10$; we
122 increase socio-technological inertia for all controls to $\dot{\alpha} = 1/90 \text{ years}^{-1}$; we set initial mitigation to $M_0 = 3\%$; and we remove
123 all "readiness" constraints, $t_\alpha = 2020$. Additionally, in order to match the mitigation cost curves in their Figure 1 S4, we found
124 it necessary to decrease the mitigation cost exponent from 2 to 1.8, as compared to 2.8 in DICE-2013 (10) or 2.6 in DICE-2016
125 (11).

126 Figure S4 shows the results of cost-benefit analysis for: a baseline scenario, a mitigation only scenario, a mitigation and CDR
127 scenario, and a scenario with mitigation, CDR, and SRM. Figure S4 has been formatted exactly as Figure 4 of Belaia (2019; 8),
128 which presents the results from equivalent simulations in their extension of DICE, for convenient side-by-side comparison.

129 **B. Soldatenko and Yusupov (2018): Analytical control theory applied to solar radiation modification.** Soldatenko and Yusupov
130 (2018; 9) develop an analytical model for the optimally cost-effective time-dependent deployment of solar radiation modification
131 (SRM) which keeps temperatures in all years below $T^* = T_0 + 1 \text{ }^\circ\text{C}$ and keeps temperatures at their end date of 2100 below T_0 .
132 Although their representation of SRM forcing is more involved than ours and depends on the mass of sulfate aerosol injected,
133 the resulting optimization problem is remarkably similar to an SRM-only configuration of the default MARGO model.

134 To approximate Soldatenko and Yusupov (2018)’s analytical model (9), we make the changes to MARGO’s default parameter
135 values reported in Table S2. Additionally, we omit adaptation, carbon dioxide removal, and mitigation, $A_{\max} \equiv R_{\max} \equiv$

Parameter	Belaia (2019)	Soldatenko and Yusupov (2018)
t_0		
t_f	2500	2100
δt	1 year	1 year
c_0		
T_0		
a		
r	75%	
B	$0.8 \times 1.13 \text{ W m}^{-2} \text{ K}^{-1}$	
κ	$0.75 \times 0.72 \text{ W m}^{-2} \text{ K}^{-1}$	
C_D	$0.75 \times 106 \text{ W yr m}^{-2} \text{ K}^{-1}$	
β		
ρ	1.5%	
E_0		
γ		
C_A		
C_R		
\tilde{C}_M	3.6% (of GWP)	
\tilde{C}_G	12.5% (of GWP)	
F_∞	7.5 Wm^{-2}	

Table S2. Values of the 19 free parameters that characterize the MARGO model, modified to replicate results from other models. Blank cells denote parameters that are not changed from the default values in Table S1.

136 $M_{\max} \equiv 0$; we remove all "readiness" constraints, $t_\alpha = 2020$, we set $T^* = 2.1 \text{ }^\circ\text{C}$ ($1 \text{ }^\circ\text{C}$ above T_0) and add an additional constraint
137 $T_{M,R,G} < T_0$ on the final timestep at $t_f = 2100$ (the latter is the only modification that required modifying compiled model
138 source code).

139 Figure S5 shows the result of cost-effectiveness optimization for an SRM-only scenario, which is formatted to be directly
140 comparable to Figure 3 of (9).

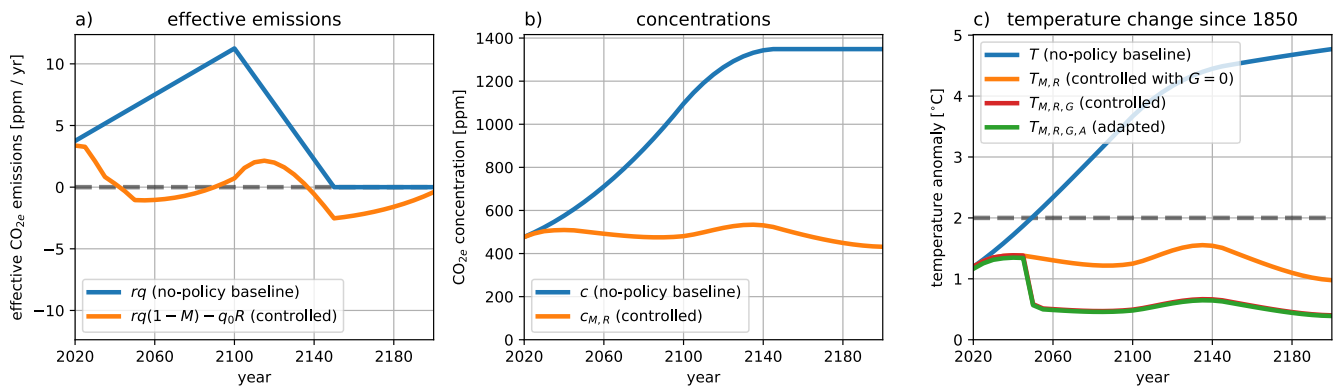


Fig. S1. Baseline (blue) and optimally-controlled (orange) a) effective CO_{2e} emissions, b) CO_{2e} concentrations, and c) temperature anomaly relative to preindustrial from cost-benefit analysis. Panel c) shows the optimal temperature change that would occur: in a baseline scenario (blue); with just emissions **Mitigation** and carbon dioxide **Removal** (orange); with **Mitigation**, **Removal**, and solar-**Geoengineering** (red); and as an “adapted temperature” with **Adaptation** measures also taken into account. The dashed grey line marks 2 °C for context. In (c), $T_{M,R,G}$ and $T_{M,R,G,A}$ decrease dramatically in 2050 relative to $T_{M,R}$ as moderate levels of SRM become permissible.

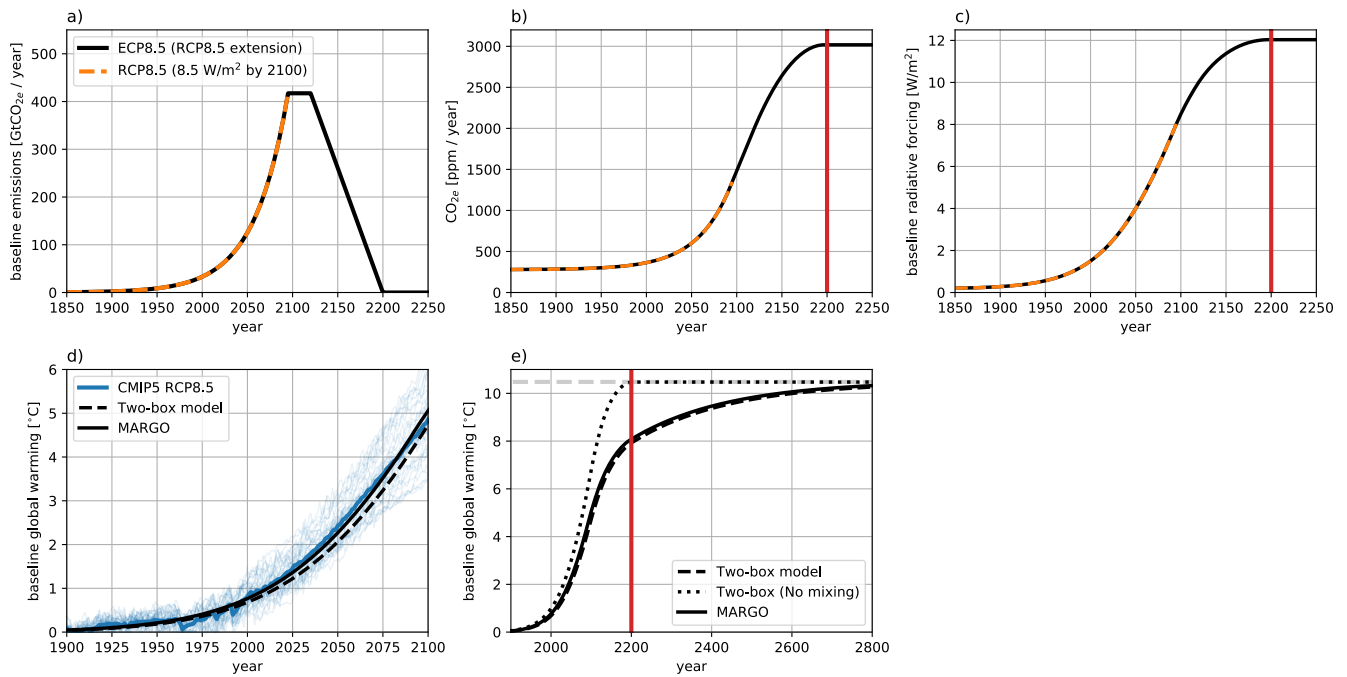


Fig. S2. Validation of the 21st Century and equilibrium responses of the MARGO Energy Balance Model (EBM). a) Baseline CO_{2e} emissions, b) concentrations, and c) radiative forcing in an RCP8.5-like scenario (dashed orange line) and its extension beyond 2100 (ECP8.5; solid black line). d) The temperature response of CMIP5 models to the RCP8.5 forcing scenario (thin blue lines for individual models; thick blue line for multi-model mean) and of the MARGO-EBM to the RCP8.5-like scenario. The dashed black line shows the full solution to the two-layer equations 2 and 3 with the same parameter values (Geoffroy 2013; 3) as the approximate solution 1 used in the MARGO-EBM. e) The temperature response to the ECP8.5 scenario for: the MARGO-EBM (solid), the full two-box model (dashed black line) and the full two-box model with $\kappa = 0$ (dotted line). The vertical red lines delineate 2200, the year in which the ECP8.5 emissions reach net zero and concentrations are stabilized.

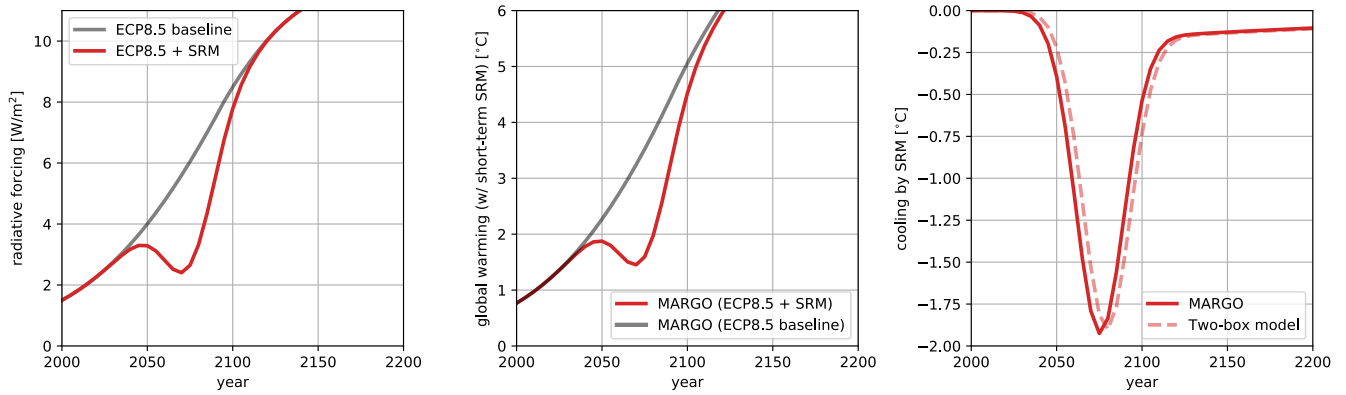


Fig. S3. Response of the MARGO-EBM to the ECP8.5 scenario (grey) and to an additional short-term variation in forcing caused by a Gaussian deployment of SRM (red). a) Radiative forcing; b) Temperature response; c) Anomalous cooling in SRM scenario relative to the ECP8.5 baseline in MARGO (solid line) and the full solution to the two-box model (dashed line).

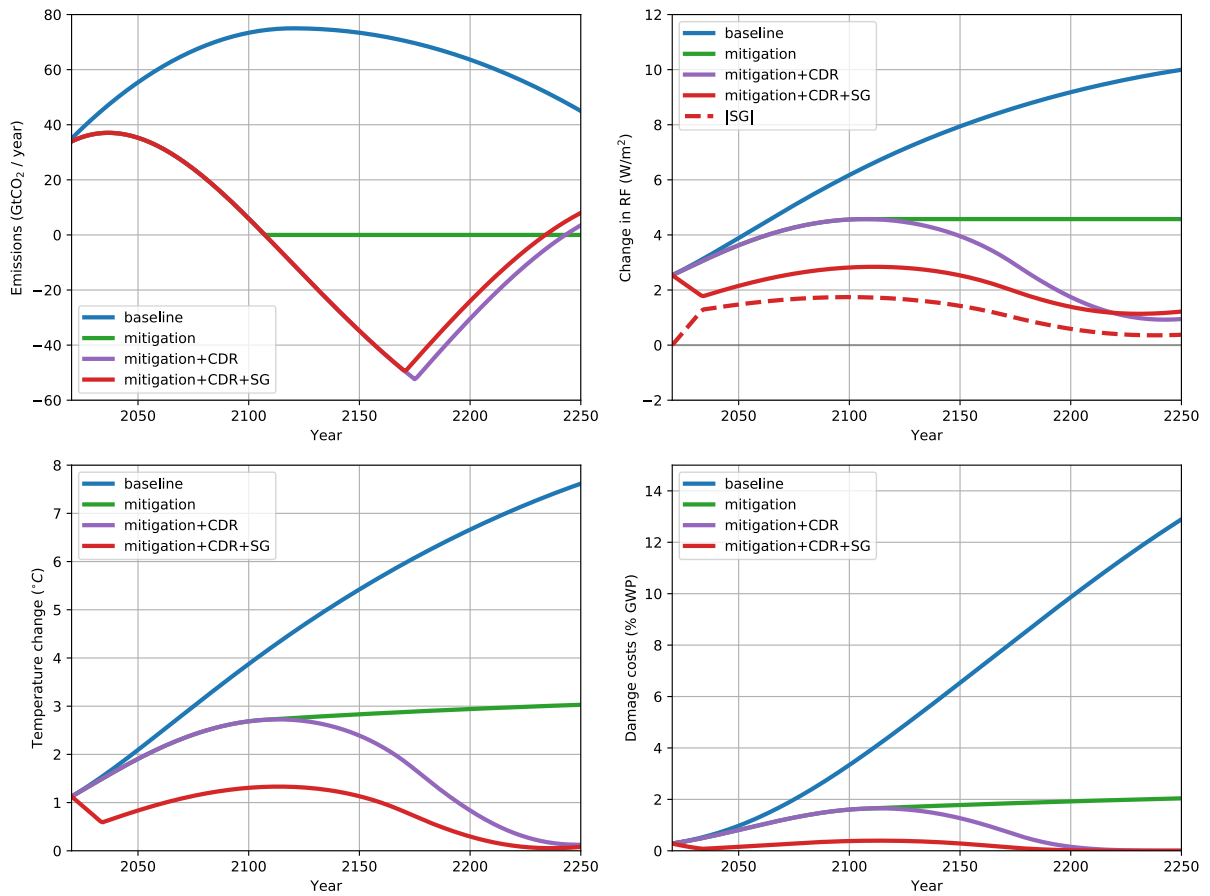


Fig. S4. A qualitative replication of Figure 4 of Belaia (2019; 8); see their figure caption and accompanying discussion of the results.

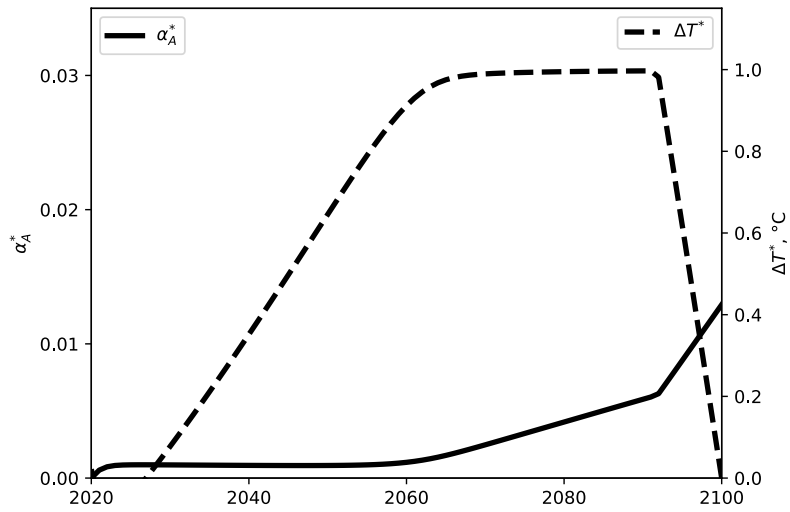


Fig. S5. A qualitative replication of Figure 3 of Soldatenko and Yusupov (2018; 9), who consider the optimally cost-effective deployments of SRM which satisfy the following temperature constraints: $\Delta T^*(t) \leq 1^\circ\text{C}$ and $\Delta T^*(t_f) \leq 0^\circ\text{C}$, where $\Delta T^* \equiv T_{M,R,G} - T_0$ is the temperature anomaly relative to 2020 (ignoring mitigation and CDR, $M \equiv R \equiv 0$) and $t_f = 2100$ is the final date. The dashed curve shows the optimal SRM albedo $\alpha_A^* \equiv \frac{G(t)F_\infty}{S_0/4}$ and the solid black line shows the temperature anomaly ΔT^* .

141 **References**

- 142 1. K Riahi, A Grübler, N Nakicenovic, Scenarios of long-term socio-economic and environmental development under climate
143 stabilization. *Technol. Forecast. Soc. Chang.* **74**, 887–935 (2007).
- 144 2. M Meinshausen, et al., The RCP greenhouse gas concentrations and their extensions from 1765 to 2300. *Clim. Chang.*
145 **109**, 213 (2011).
- 146 3. O Geoffroy, et al., Transient Climate Response in a Two-Layer Energy-Balance Model. Part I: Analytical Solution
147 and Parameter Calibration Using CMIP5 AOGCM Experiments. *J. Clim.* **26**, 1841–1857 (2012) Publisher: American
148 Meteorological Society.
- 149 4. R Calel, DA Stainforth, On the Physics of Three Integrated Assessment Models. *Bull. Am. Meteorol. Soc.* **98**, 1199–1216
150 (2016) Publisher: American Meteorological Society.
- 151 5. K Dow, et al., Limits to adaptation. *Nat. Clim. Chang.* **3**, 305–307 (2013) Number: 4 Publisher: Nature Publishing Group.
- 152 6. SC Sherwood, M Huber, An adaptability limit to climate change due to heat stress. *Proc. Natl. Acad. Sci.* **107**, 9552–9555
153 (2010) Publisher: National Academy of Sciences _eprint: <https://www.pnas.org/content/107/21/9552.full.pdf>.
- 154 7. JA Flegal, AM Hubert, DR Morrow, JB Moreno-Cruz, Solar Geoengineering: Social Science, Legal, Ethical, and Economic
155 Frameworks. *Annu. Rev. Environ. Resour.* **44**, 399–423 (2019) _eprint: <https://doi.org/10.1146/annurev-environ-102017-030032>.
- 156 8. M Belaia, Optimal Climate Strategy with Mitigation, Carbon Removal, and Solar Geoengineering. *arXiv:1903.02043*
157 [*econ, q-fin*] (2019) arXiv: 1903.02043.
- 158 9. SA Soldatenko, RM Yusupov, Optimal Control of Aerosol Emissions into the Stratosphere to Stabilize the Earth’s Climate.
159 *Izvestiya, Atmospheric Ocean. Phys.* **54**, 480–486 (2018).
- 160 10. W Nordhaus, P Sztorc, Dice 2013r: Introduction and user’s manual. *Yale Univ. Natl. Bureau Econ. Res. USA* (2013).
- 161 11. WD Nordhaus, Revisiting the social cost of carbon. *Proc. Natl. Acad. Sci.* **114**, 1518–1523 (2017) Publisher: National
162 Academy of Sciences Section: Social Sciences.
163